Laser feedback interferometry and applications: a review

Jiyang Li
Haisha Niu
Yanxiong Niu

Laser feedback interferometry and applications: a review

Jiyang Li, Haisha Niu, and Yanxiong Niu*
Beihang University, School of Instrumentation Science and Optoelectronics Engineering, Beijing, China

Abstract. The progress on laser feedback interferometry technology is reviewed. Laser feedback interferometry is a demonstration of interferometry technology applying a laser reflected from an external surface, which has features including simple structure, easy alignment, and high sensitivity. Theoretical analysis including the Lang–Kobayashi model and three-mirror model are conducted to explain the modulation of the laser output properties under the feedback effect. In particular, the effect of frequency and polarization shift feedback effects are analyzed and discussed. Various applications on various types of lasers are introduced. The application fields range from metrology, to physical quantities, to laser parameters and other applications. The typical applications of laser feedback technology in industrial and research fields are discussed. Laser feedback interferometry has great potential to be further exploited and applied. © *2017 Society of Photo-Optical Instrumentation Engineers (SPIE)* [DOI: 10.1117/1.OE.56.5.050901]

1 Introduction

Laser feedback interferometry, or self-mixing interferometry, is a demonstration of interferometry technology applying a laser reflected from an external surface.[1] Unlike traditional laser interferometry, laser feedback interferometry does not need additional optical elements for inducing interference outside the laser cavity.[2] Instead, self-mixing interference occurs inside the laser cavity. The laser feedback phenomena can easily be caused by any surface in the light paths of the optical systems. Previously, laser feedback phenomena was regarded as damaging to the laser's performance because it induced instability in the laser power and frequency or caused strong quantum noises and coherent collapse.[3] However, since its application by King and Steward as a displacement sensor in 1963,[4,5] a massive amount of both theoretical and experimental work has been done in the field of laser feedback interferometry. According to laser feedback theory, laser intensities, polarization states, and phase behavior of lasers can be modified by introducing coherent optical feedback from external surfaces. Also, the bandwidth of the lasers can be enhanced or compressed under the laser feedback effect.

As long as the electromagnetic wave emitted is reinjected back into the laser cavity, self-mixing interference will be caused.[6] The laser feedback effect is a remarkably universal phenomenon that can be observed in lasers of all different types. Among the work reported before, the laser feedback effect has been observed in gas lasers,[7] semiconductor diode lasers,[8] solid-state lasers,[9,10] vertical-cavity surface-emitting lasers (VCSELs),[11] mid-infrared lasers,[12] and terahertz quantum cascade lasers (THZ QCLs),[13] as well as in interband cascade lasers,[14] fiber[15] and fiber ring lasers,[16] micro ring lasers,[17] and quantum dot lasers.[18]

Compared to traditional laser interferometry, laser feedback interferometry has inherent advantages. The structure is more compact with fewer optical elements, the optical setup is easier for alignment, the laser feedback signal is detectable everywhere on the beam, and the beam at the target side can be exploited in special applications. Since laser feedback interferometers have no limits on the types of lasers, a variety of lasing wavelengths and bandwidths can be realized. The laser feedback interferometer can operate on a normal diffusing target surface due to its high sensitivity. Above all, with the growing need for precise measurement under various conditions, laser feedback interferometry is becoming more and more widely applied.[19]

This paper aims to provide an overall view of laser feedback interferometry. The framework of the paper is structured as follows. Section 2 reveals the theoretical analysis of laser feedback interferometry. Together with traditional laser feedback, the scheme and principles of the frequency-shifted and polarization-shifted laser feedback are proposed. Section 3 is an overview of the laser feedback effect on applications in metrology, including displacement, vibration, distance, velocity, angle, and thickness measurement. Section 4 reveals laser feedback interferometry used for laser parameters measurement, such as linewidth, line width enhancement factor, and polarization cross-saturation coefficient. In Sec. 5, the measurement of physical quantities is discussed, including refractive index, internal stress, thermal expansion coefficient, evaporation rate of liquid, and acoustic field distribution. In Sec. 6, applications including confocal tomography and imaging technology, sound rehabilitation, random bit generator, and chaos generator are explored. A summary and promising future directions are discussed in Sec. 7.

2 Theoretical Analysis of Laser Feedback Interferometry

The laser feedback effects in all kinds of lasers are always following the same principle. Light is emitted from the laser cavity and then transmitted to an external target. From the

*Address all correspondence to: Yanxiong Niu, E-mail: niuyx@buaa.edu.cn

surface of the target, the light is partially reflected and transmitted back into the laser cavity in the same optical path, where a portion of the light re-enters the laser cavity. Then, the reinjected light interacts with the resonant mode of the laser, and the property of the laser is modulated. Since the laser has a self-coherent nature, laser feedback systems are only sensitive to the laser reflected back to the laser cavity, suppressing most of the external radiation entering the laser cavity, which is regarded as noise in laser feedback systems. Due to the fact that all kinds of laser feedback interferometers share the same theoretical basis, the theoretical analyses are of great significance in revealing the phenomena in laser feedback effects and bringing to light potential applications.

In the transmission process, the feedback light passes through the optical path twice and is reflected by the surface of the target. Then, the reinjected light is embedded with the information of the external optical path or the property of the target. The feedback process brings the information back into the laser cavity. The interaction or the interference between the feedback light and the laser cavity causes modulations in the laser output properties, such as intensity, polarization state, working frequency, and phase position. Beam properties can be monitored by various kinds of detectors, and the information can be demodulated. Therefore, information about the target or external optical path can be easily obtained in a highly sensitive way. To fulfill precise demodulation of the information in the feedback light, theoretical analyses need to be carried out. Below are the two most commonly used methods for analyzing the laser feedback effect. Also, the effects of frequency and polarization shift feedback are discussed as important research foci to be explored further.

2.1 Lang–Kobayashi Model and Three-mirror Model

Lang and Kobayashi[20] reported the laser feedback effect in laser diodes. They analyzed the multistable and hysteresis phenomena in laser diodes and put forward a theoretical solution by defining the degree of matching between the external feedback cavity and the laser resonant cavity. A component representing the effect of the external feedback in the form of a complex number has been added to the rate equations of diode lasers, which is known as the famous Lang–Kobayashi model. The proposal of this model has laid a solid foundation for the following studies.

The space between the output mirror of the laser cavity and the surface of the object is called the laser external feedback cavity. If the coupling strength between the laser cavity and the external cavity is κ, the standard Lang–Kobayashi equation can be expressed as follows:[21–25]

$$\frac{d}{dt}[E(t)e^{j\omega t}] = \left\{ j\omega_m + \frac{1}{2}\left(\Gamma G - \frac{1}{\tau_p}\right) \right\} \times E(t)e^{j\omega t} + \tilde{\kappa}E(t - \tau_{\text{ext}})e^{j\omega(t - \tau_{\text{ext}})}, \tag{1}$$

where $E(t)$ is the scaled, slowly varying complex envelope of the electric field; ω is the laser mode angular velocity; t is the time; ω_{m} is the cavity resonance angular frequency; Γ is the optical confinement factor; G is the gain in the laser cavity; τ_p is the photon lifetime in the laser cavity; τ_{ext} is the external feedback cavity round-trip time; and $\tilde{\kappa}$ is the feedback

coupling rate, meaning the reinjected light is coupled into the laser cavity at this rate, which can be expressed as follows:

$$\tilde{\kappa} = \kappa \frac{1}{\tau_{\text{in}}}. \tag{2}$$

The gain term G is also related to another variation, which is the carrier density N. It can be expressed as follows:

$$\frac{dN(t)}{dt} = \frac{\eta_i I(t)}{qV} - \frac{N(t)}{\tau_n} - GS(t), \tag{3}$$

where η_i is the current injection efficiency of the laser diodes, I is the laser driving current, q is the charge of an electron, V is the cavity volume, τ_n is the carrier lifetime, and S is the photon density in the laser cavity. Equation (1) together with Eq. (3) describes the laser diodes dynamics under optical feedback.

Performing the differentiation of the product on the left side of Eq. (1), it can be deduced as follows:

$$\frac{dE(t)}{dt} = \left\{ j(\omega_{\text{m}} - \omega) + \frac{1}{2}\left(\Gamma G - \frac{1}{\tau_p}\right) \right\} \times E(t) + \tilde{\kappa}E(t - \tau_{\text{ext}})e^{-j\omega\tau_{\text{ext}}}. \tag{4}$$

In order to obtain the phase property through the rate equations, the phase $\varphi(t)$ of the scaled, slowly varying complex envelope of the electric filed $E(t)$ is defined as follows:

$$\varphi(t) = \arctan\left\{ \frac{\text{Im}[E(t)]}{\text{Re}[E(t)]} \right\}. \tag{5}$$

Combining Eqs. (4) and (5), the phase can be expressed as follows:

$$\frac{d\varphi(t)}{dt} = (\omega_{\text{m}} - \omega) - \tilde{\kappa}\left[\frac{S(t - \tau_{\text{ext}})}{S(t)}\right]^{\frac{1}{2}} \times \sin[\omega\tau_{\text{ext}} + \varphi(t) - \varphi(t - \tau_{\text{ext}})]. \tag{6}$$

Using the linewidth enhancement factor α, which is defined as the ratio of change in the real part of the laser refractive index to the change in the imaginary part of the laser refractive index, Eq. (6) can be deduced as follows:

$$\frac{d\varphi(t)}{dt} = \frac{1}{2}\alpha\left(\Gamma G - \frac{1}{\tau_p}\right) - \tilde{\kappa}\left[\frac{S(t - \tau_{\text{ext}})}{S(t)}\right]^{\frac{1}{2}} \times \sin[\omega\tau_{\text{ext}} + \varphi(t) - \varphi(t - \tau_{\text{ext}})]. \tag{7}$$

The Lang–Kobayashi model is time-dependent and can be used to describe the dynamic properties of active materials. It is found to give a remarkably accurate modeling of both the weak-level feedback phenomena and the high-level feedback chaos-related dynamics. Although it is deduced on the basis of the performance on laser diodes, it predicts many complex behaviors over short-time scales that have been observed in practice. In contrast to the dynamic Lang–Kobayashi model, there also exists another way of analyzing the laser feedback effect, which employs the geometry of the laser feedback cavity and effective reflectivity. Unlike the
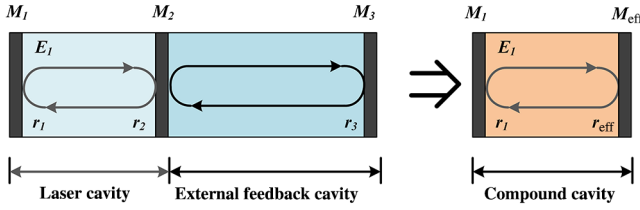
Fig. 1 The schematic diagram of three-mirror model in the laser feedback system. (a) The standard three-mirror model. (b) The simplified model of the compound cavity. M_1, M_2, mirrors of the resonant cavity; M_3, the equivalent reflective mirror of the target; M_{eff}, the compound reflective mirror of M_2 and M_3.

dynamic description obtained by adding the feedback effect component in the rate equations as in the Lang–Kobayashi model, the three-mirror model employs the static analysis method. The three-mirror model is equivalent to the Lang–Kobayashi model in analyzing the phenomena in the laser feedback technology, but the analysis processes of the two models focus on different aspects. de Groot[26] proposed the three-mirror model, which explains the feedback effect in the aspect of the laser output intensity. The key point in the three-mirror model is to treat the reflective target as the third reflective mirror. This reflective mirror reflects the laser back into the resonant cavity, equivalent to changing the effective reflectivity of the laser output mirror, which induces modulation of the optical field inside the laser cavity. The schematic diagram is shown in Fig. 1.

Suppose the electric field inside the laser cavity is $E_1(t)$; the electric field reflected by the laser cavity M_2 is $E_2(t) = E_1(t)r_2$, whereas the electric field output of the laser cavity is $E_{ext}(t) = E_1(t)\sqrt{1 - r_2^2}$. The electric field transmitting through the external feedback cavity and back to the laser cavity can be expressed as[27,28]

$$E_{ext}(t - \tau_{ext}) = E_1(t - \tau_{ext})\sqrt{1 - r_2^2} \times \exp(-j2\pi\nu\tau_{ext}) \times \kappa,$$
(8)

where ν is the laser frequency; since the external feedback cavity round-trip time τ_{ext} is in a small scale, approximation can be done with $E_1(t - \tau_{ext}) \cong E_1(t)$. The compound reflected electric field can be expressed as

$$\begin{aligned} E_{eff}(t) &= E_1(t)r_2 + E_{ext}(t) \\ &= E_1(t)r_2 + E_1(t)\sqrt{1 - r_2^2} \times \exp(-j2\pi\nu\tau_{ext}) \times \kappa \\ &= E_1(t)[r_2 + (1 - r_2^2) \times \exp(-j2\pi\nu\tau_{ext}) \times \kappa] \\ &= E_1(t)r_2[1 + \kappa_{ext} \exp(-j\phi)], \end{aligned}$$
(9)

where $\kappa_{ext} = (1 - r_2^2)\kappa/r_2$ is the equivalent electric field feedback coefficient and $\phi = 2\pi\nu\tau_{ext}$ is the phase shift under the feedback effect. From Eq. (9), the equivalent reflective index can be expressed as follows:

$$r_{eff} = \frac{E_{eff}}{E_1} = r_2[1 + \kappa_{ext} \exp(-j\phi)].$$
(10)

In ordinary lasers, $|r_1|^2 = 1$ and $|r_2|^2 \approx 1$. The optical field loss rate γ_c can be expressed as follows:

$$\gamma_c = \frac{c}{2nL} \ln\left(\frac{1}{|r_1|^2|r_2|^2}\right) \approx \frac{c}{2nL}(1 - |r_2|^2).$$
(11)

Under the laser feedback effect, the reflective index r_2 can be replaced by r_{eff}, such that the optical field loss rate with laser feedback influence γ_c^{eff} can be expressed as follows:

$$\gamma_c^{eff} \approx \frac{c}{2nL}(1 - |r_{eff}|^2) \approx \gamma_c - 2\gamma_c\kappa \exp(-j\phi).$$
(12)

The initial rate equations in the laser can be expressed as

$$\begin{aligned} \frac{dN}{dt} &= \gamma(N_0 - N) - BN|E|^2, \\ \frac{dE(t)}{dt} &= \left[j(\omega_m - \omega) + \frac{1}{2}(BN - \gamma_c)\right]E(t), \end{aligned}$$
(13)

where N_0 is the inversion particle number under a small signal, γ is the inversion particle loss rate, and B is the stimulated radiation coefficient. The rate equations under the laser feedback effect can be expressed as follows:

$$\begin{aligned} \frac{dN}{dt} &= \gamma(N_0 - N) - BN|E|^2, \\ \frac{dE(t)}{dt} &= \left[\frac{1}{2}(BN - \gamma_c) + j(\omega_m - \omega)\right]E(t) + \gamma_c\kappa\cos(\phi)E(t). \end{aligned}$$
(14)

Comparing Eqs. (13) and (14), it can be seen that, under the effect of laser feedback, the intensity of the laser output has been added with a modulation component, while the phase ϕ can be defined as

$$\tan\phi = \frac{\kappa_{ext}\sin(4\pi L_{ext}/\lambda)}{1 + \kappa_{ext}\cos(4\pi L_{ext}/\lambda)},$$
(15)

where L_{ext} is the external cavity length. With Eqs. (9) and (15), by the approximation method, the intensity of the laser output under the laser feedback effect can be expressed as follows:

$$I = I_0 - \kappa_{ext}\cos\left(\frac{4\pi L_{ext}}{\lambda}\right).$$
(16)

From Eq. (16), I_0 is the laser intensity without the laser feedback effect. Under the laser feedback effect, a cosinoidal modulation is added in the intensity. Every half of the wavelength change in the external cavity length corresponds to one cycle in the intensity modulation. The three-mirror model is especially appropriate for analyzing the intensity modulation in the laser feedback field. Both the Lang–Kobayashi model and the three-mirror model can explain the feedback phenomena in various types of lasers, e.g., gas lasers, semiconductor diode lasers, solid-state lasers, and VCSELs. Therefore, both models are effective tools in the research of laser feedback interferometry.

2.2 Laser Feedback Effect with Frequency Shift and Polarization Shift

In the above section, the effect of single-frequency and single-polarization feedback is discussed in the two models.

However, to improve the performance of lasers under the laser feedback effect and expand its applications, the feedback effects with different properties are discussed in this section.

2.2.1 Frequency-shifted feedback

In the laser feedback system, frequency shift technology can also be applied to improve the performance of the laser feedback interferometers. When the frequency shift modulator is added inside the external feedback cavity of the laser, the model of the frequency-shifted laser feedback system is shown in Fig. 2. The frequency of the laser output is ν, and the frequency shift of the modulator is Ω. Since the light reinjected into the laser cavity transmits through the frequency shifter twice, the feedback laser has the frequency of $\upsilon + 2\Omega$.

Under the effect of the frequency-shifted feedback, Eq. (8) can be rewritten as follows:

$$E_{\text{ext}}(t - \tau_{\text{ext}}) = E_1(t - \tau_{\text{ext}})\sqrt{1 - r_2^2}$$
$$\times \exp[-j2\pi(\nu + 2\Omega)\tau_{\text{ext}}] \times \kappa. \quad (17)$$

The rate equations under frequency-shifted feedback can be expressed as follows:[29]

$$\frac{dN}{dt} = \gamma(N_0 - N) - BN|E|^2,$$
$$\frac{dE(t)}{dt} = \left[\frac{1}{2}(BN - \gamma_c) + j(\omega_{\text{m}} - \omega)\right]E(t)$$
$$+ \gamma_c\kappa \exp(j2\Omega) \exp[-j(\omega + 2\pi\Omega)\tau_{\text{ext}}]E(t). \quad (18)$$

With Eqs. (17) and (18), the relative modulation of the laser intensity is expressed as

$$\frac{\Delta I(2\Omega)}{I_s} = \kappa G(2\Omega) \cos(2\Omega t - \phi + \phi_{\text{s}}), \quad (19)$$

where $\Delta I(2\Omega)$ is the modulation under the frequency-shifted laser feedback effect, I_{s} is the stable laser output intensity, ϕ_{s} is the fixed additional phase, and $G(2\Omega)$ is the gain factor. In some types of lasers, such as solid-state lasers or semiconductor lasers, there exists the relaxation oscillation phenomenon. In these continuous-functioning lasers, the output light is made up of spike pulses instead of smooth pulses.[30] The relaxation oscillation phenomenon is caused by the dynamic interaction between the radiation inside the laser resonant cavity and energy storage in the laser medium. If the relaxation oscillation frequency of the laser is ν_{R}, the gain factor
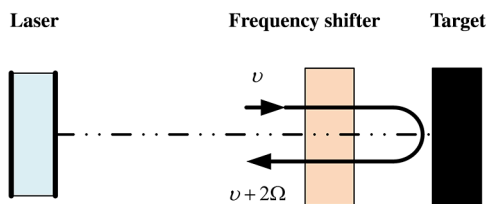
$G(2\Omega)$ in the solid-state laser is a function of the oscillation phenomenon frequency ν_{R}, which can be expressed as

$$G(2\Omega) = 2\gamma_c \frac{[\eta^2\gamma^2 + (2\Omega)^2]^{\frac{1}{2}}}{\{\eta^2\gamma^2(2\Omega)^2 + [\nu_R^2 - (2\Omega)^2]^2\}^{\frac{1}{2}}}, \quad (20)$$

where η is the pumping level. This gain factor is a unique property in the frequency-shifted feedback systems. This gain factor equals the amplification in the laser feedback signal. From Eq. (20), when 2Ω equals ν_{R}, the gain factor $G(2\Omega)$ reaches its maximum value. Then, Eq. (20) can be deduced as follows:

$$G(2\Omega) = 2\gamma_c \frac{[\eta^2\gamma^2 + (\nu_R)^2]^{\frac{1}{2}}}{[\eta^2\gamma^2(\nu_R)^2]^{\frac{1}{2}}} = 2\frac{\gamma_c}{\eta\gamma} \cdot \frac{[\eta^2\gamma^2 + (\nu_R)^2]^{\frac{1}{2}}}{\nu_R}. \quad (21)$$

Since the relaxation oscillation frequency of the laser is relatively large in amount, it can be seen that $\eta^2\gamma^2 \ll \nu_R^2$, $[\eta^2\gamma^2 + (\nu_R)^2]^{\frac{1}{2}} \cong \nu_R$, then Eq. (21) can be simplified as

$$G(2\Omega) \cong \frac{2}{\eta}(\gamma_c/\gamma). \quad (22)$$

For the solid-state lasers, this maximum gain factor value can reach to a scale as high as 10^6, indicating that the solid-state laser frequency-shifted feedback system has ultrahigh sensitivity for the feedback light. Once the proper shift frequency is set, the feedback light can be greatly amplified, which makes the solid-state laser frequency-shifted feedback system extremely appropriate for weak signal detection.

2.2.2 Polarization-shifted feedback

By adding a birefringence component into the laser feedback cavity, the polarization states of the feedback light can be shifted and the laser output intensities in the two orthogonal directions with the phase difference can be modulated.[31–34] The birefringence components are usually in the form of wave plates or quartz crystals. When the birefringence component is put into the external cavity, the original external cavity forms two different physical external cavities. Supposing the two axes in the laser are x and y, the birefringence axes in the birefringent component are in the same directions. Also suppose the amplitude reflection coefficients of both laser cavity mirrors are r_1 and r_2; the transmission coefficient of the laser is $T = 1 - r_2^2$; r_3 is the reflection coefficient of the feedback mirror; l is the length of the external cavity; and in the corresponding axes, the external cavity lengths are l_{o} and l_{e}, d is the length of laser cavity, n is the refractive index of the laser material, and ξ is the feedback coefficient. Then, the gain of the laser in the x and y axes is as follows:

$$\begin{cases} g_x = -\frac{1}{nd}\left[\ln(r_1 r_2) + \frac{\beta}{2}\cos\varphi\right], \\ g_y = -\frac{1}{nd}\left[\ln(r_1 r_2) + \frac{\beta}{2}\cos(\varphi + 2\delta)\right], \end{cases} \quad (23)$$

where $\beta = Tr_3\xi/r_2$ and $\varphi = 4\pi\upsilon l_o/c$, δ is the phase difference of the birefringence component. Under the effect of the polarization-shifted feedback, the laser intensities in two orthogonal axes can be expressed as

Fig. 2 The model of the frequency-shifted laser feedback system. ν, the frequency of the laser output; Ω, the frequency shift of the modulator.

$$\begin{cases} I_x = I_{0x}\left[1 + \frac{\beta K}{2nd}\cos\varphi\right] \\ I_y = I_{0y}\left[1 + \frac{\beta K}{2nd}\cos(\varphi + 2\delta)\right] \end{cases}, \qquad (24)$$

where I_0 is the initial intensity without feedback and K is the constant. From Eq. (24), the intensities have a phase difference that is twice the phase difference of the birefringence component. As a result, the polarization-shifted feedback effect can be utilized to measure the birefringence, optic axis azimuth,[35] or displacement.[36]

The above models and analyses give theoretical explanations of the corresponding relationship between the external feedback cavity and the variations in the parameters inside the laser cavity. By applying this correspondence relationship, various kinds of applications can be fulfilled with laser feedback interferometry. Below are some typical applications of the laser feedback effect. In order to simplify the interferometer structure and reduce the cost, the laser sources in these self-mixing laser interferometers are mostly commercial semiconductor lasers with photodetectors sealed inside. In some special occasions, the lasers are solid-state lasers, gas lasers, or other lasers. In fields needing precision measurement, the stability of the laser frequency is required, since the cycles of the laser feedback signals are directly traced back to the laser wavelength. Instabilities in laser power and frequency will bring errors in the measurement results. Therefore, the laser stability and robustness are required for laser feedback interferometers.

3 Laser Feedback Technology Applications in Metrology

Metrology is the science of measurement, embracing both experimental and theoretical determinations at any level of uncertainty in any field of science and technology. As the basic research in the measurement field, precise measurement is significant and can be applied in a large variety of fields. On the basis of the theoretical analyses above, six typical aspects of laser feedback effect applications in metrology are described in the following sections.

3.1 Displacement Measurement

In the fields of metrology, the precise measurement of displacement has always been a research focus. Since the displacement measurement is widely applied in various industrial situations and scientific research, noncontact measurements are in strong demand. Compared with traditional laser interferometers, the laser feedback interferometer has great potential because it does not need a retroreflector and can be applied to a nonmatching target with a diffuse or rough surface. In the above analyses of laser feedback theory, according to Eq. (16), every change of half the wavelength in the length of the external cavity corresponds to a cycle in the laser intensity modulation. The congruent relationship makes it easy to measure displacement by counting the total cycles of modulation.

With the rapid development of displacement measurement based on laser feedback technology, various methods emerge, such as fringe counting technology with its simple structure and high sensitivity.[37] The method makes use of fringe counting technology since half of the wavelength distance change in the external cavity corresponds to a cycle of intensity modulation in the laser feedback effect. The

directions of dips in the sawtooth-shaped feedback waveforms indicate the direction of the displacement. The method is capable of measuring displacement in half of the wavelength scale on a substantial distance up to 1 m without any optical adjustment aside from the initial pointing on the target.

A research focus of laser feedback technology applied in the displacement measurement field is the heterodyne microchip solid-state laser employing external frequency-shifted feedback.[38,39] As mentioned above, the relaxation oscillation phenomenon in solid-state lasers causes a highly sensitive response as large as 10^6 to the frequency-shifted laser feedback. The schematic diagram is shown in Fig. 3.

As shown in Fig. 3, the microchip laser is a laser diode pumped Nd:YAG or Nd:YVO$_4$ laser and is frequency stabilized by precise control of the temperature.[40] The feedback levels are studied and ensured for the performance of the interferometers. The acousto-optic modulators are used to produce the shift in the frequency of the laser reinjected back into the laser cavity. Since the working frequency of the acousto-optic modulator is usually high, two acousto-optic modulators are employed, and the frequency difference between them is used as the feedback frequency shift. Suppose the working frequency of the AOM$_1$ and AOM$_2$ is Ω_1 and Ω_2, respectively, Ω is the difference between Ω_1 and Ω_2. The schematic diagram of the optical path is shown in Fig. 4.

Due to the frequency shift characteristics of the acousto-optic modulators, the laser reflected by the target can obtain a frequency shift of 2Ω in the measurement signal, while the laser reflected by the reference mirror can obtain a frequency
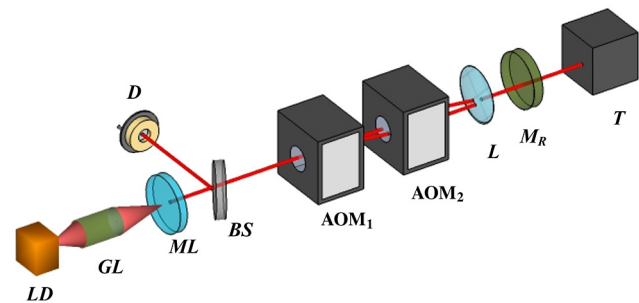

Fig. 3 Schematic configuration of the frequency-shifted laser feedback interferometer. LD, laser diode; GL, grin lens; ML, microchip laser; BS, beam splitter; D, detector; AOMs, acousto-optic modulators; L, lens; M$_R$, reference mirror; T, target.
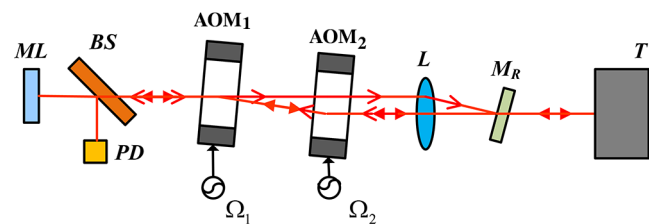

Fig. 4 Schematic diagram of the optical path in the frequency-shifted feedback interferometer. ML, microchip laser; BS, beam splitter; PD, photodetector; AOM, acousto-optic modulators; L, lens; M$_R$, reference mirror; T, target.

shift of Ω acting as the reference signal. The analyses are as follows: The optical path of the reference beam is shown in hollow arrows while the measurement beam is in solid arrows. If the frequency of the initial light emitted is v, the reference beam passes the acousto-optic modulators AOM_1 and AOM_2 without diffraction, which means the frequency remains v. The measurement beam passes through AOM_1 and is diffracted at -1 order, which means the frequency is $v - \Omega_1$; then it passes through AOM_2 and is diffracted at $+1$ order such that the frequency now is $v - \Omega_1 + \Omega_2 = v + \Omega$. The reference beam is focused by lens L and reflected back to the acousto-optic modulators, and then it is diffracted at $+1$ order in AOM_2 and at -1 order in AOM_1, while the measurement beam is reflected at the target surface and is diffracted again at $+1$ order in AOM_2 and at -1 order in AOM_1. As a result, the feedback reference beam has the frequency of $v - \Omega_1 + \Omega_2 = v + \Omega$, whereas the feedback measurement beam has the frequency of $v - \Omega_1 + \Omega_2 + \Omega_2 - \Omega_1 = v + 2\Omega$. The displacement information in both the measurement signal and reference signal is demodulated, and the displacement detected in the reference signal is used for compensation. Therefore, the frequency-shifted laser feedback interferometer can achieve high resolution and accurate displacement measurement with little zero drift. The resolution of the frequency-shifted laser feedback interferometer is 1 nm by phase discrimination method, and the zero drift within 3 min is less than 8 nm.[39] The performance of the laser feedback frequency shift interferometer is calibrated, compared with the commercial dual-frequency laser interferometer Agilent 5529A. The correlation coefficient of the linear fit differs from 1 by 6×10^{-4}, and the residual error is <1.5 μm.

The method has relatively high resolution and sensitivity due to the frequency-shifted feedback characteristics in solid-state lasers, as analyzed in Sec. 2. Therefore, the frequency-shifted laser feedback increases the sensitivity in the laser feedback interferometer, making it especially appropriate for measuring objects with rough and black surfaces or irregular shapes. The sensitivity is improved at the cost of a more complicated structure and increased expense. However, the measurement range is limited to about 1 m since the measurement process needs a proper feedback level,[39] and the method for determining the direction of displacement is difficult and complex to realize. Due to the fact that the common part of the measuring optical path and the referring optical path is limited, with the increasing measurement range, the accuracy will be affected. Another method is a laser feedback interferometer based on the phase difference of orthogonally polarized lights in the external birefringence cavity.[41,42] The method determines the direction of the displacement easily by the sequences of two orthogonally polarized lights. The measuring range is large, and the measurement is not limited by the feedback level. The schematic diagram is shown in Fig. 5. The laser applied is a laser diode pumped Nd : YVO$_4$ laser.

The theory of this method is as follows: when linearly polarized light passes through the birefringent external cavity and then is reflected back into the laser resonator by an external object, a phase difference is generated between the laser sinusoidal modulated intensities in the two orthogonal directions. The birefringence in the external cavity is produced by the wave plate, the phase retardation of which is 45 deg.
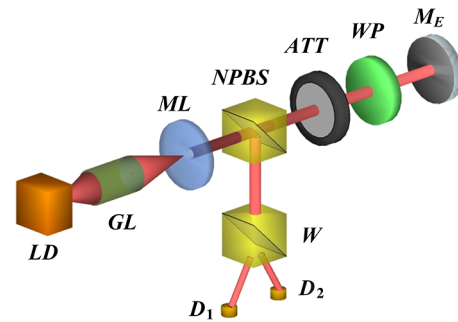

Fig. 5 Schematic diagram of laser feedback interferometer based on phase difference of orthogonally polarized lights in external birefringence cavity. LD, laser diode; GL, grin lens; ML, microchip laser; NPBS, nonpolarizing beam splitter; ATT, attenuation plate; WP, wave plate; M_E, feedback mirror; W, Wollaston prism; D_1, D_2, detectors.

A phase difference of 90 deg is induced between the two orthogonally polarized components. By applying fringe counting technology and fourfold subdivision, displacement can be easily calculated with high precision. The linearity of this system is 2.57×10^{-5} over a 7-mm range, and the standard deviation is 0.34 μm. The resolution is 53.2 nm and can be further improved by applying multifold subdivision methods adopted in the grating encoders.

In addition to the three methods mentioned above, there also exist various other methods for displacement measurement applying laser feedback technology. Guo et al.[43] reported a method based on the laser feedback grating interferometer, which applies a double-diffraction system. The operating frequency is 100 MHz, and the error is <2.9 nm. Bernal et al.[44] proposed a robust fringe detection method based on biwavelet transform. Wavelet transform is applied, and it enables the measurement of arbitrarily shaped displacements based on the pattern recognition capability. Donati et al.[45] reported a method for simultaneous measurement of displacement and tilt and yaw angles of the target, taking advantage of two orthogonal modulations of the beam. Zeng et al.[46] proposed laser feedback interferometer based on high-density cosine-like intensity fringes with phase quasi quadrature; the system has a resolution of 0.51 nm in 850 μm and the displacement measurement accuracy was 5 nm.[47] Jha et al.[48] presented a method making efficient use of direct laser injection current modulation to induce continuous wave frequency modulation and nonlinear dynamics effects in a laser diode subjected to optical feedback to measure nanometric amplitude displacements. The error is 2.4 nm. Chen et al.[49] proposed synthetic-wavelength self-mixing interferometry for displacement measurement. The virtual synthetic wavelength is 10^6 times larger than the operating wavelength, so the subnanometer displacement can be obtained.

3.2 Vibration Measurement

When the displacement to be measured is less than half the wavelength in the amplitude with a relatively high frequency range, the fringe counting method is not appropriate and not accurate enough. In the case of vibration, the amplitude is relatively small and the frequency is high, which requires different techniques from displacement measurement.

Signal processing proposed by Tao et al.[50] synthesizing wavelet transform and Hilbert transform is employed to measure uniform or nonuniform vibrations in the laser feedback interferometer based on a semiconductor laser diode with quantum well. Background noise and fringe inclination are solved by the decomposing effect, fringe counting is adopted to automatically determine the decomposing level, and a couple of exact quadrature signals are produced by Hilbert transform to extract vibration. The continuous wavelet transform is applied to weaken the inclination of the fringe. From the results, it can be seen that the reconstructed phase curve is in high accordance with the assumptive phase curve, indicating that this method has excellent performance in vibration measurement. This method has the following advantages. First, the frequency or phase modulation is deleted from the system, so the bandwidth limitation from modulation is removed; the size and cost both decrease sharply. Second, the feedback level is not limited, making it more applicable in general environments. Third, the high computational efficiency provides potential in real-time monitoring, and noise is greatly restrained.

When self-mixing interferometry occurs in an asymmetrical cavity, the light and the vibration target are not strictly vertical. The light will experience multiple reflections between the vibration target and the laser. In such cases, the number of interference fringes doubles or even increases by three or four times. This phenomenon is called multiple self-mixing interferometry.[51] Jiang et al.[52] proposed a demodulation algorithm based on the power spectral analysis for multiple self-mixing interferometry. Its precision can reach as high as $\lambda/47.6$, and the absolute error of amplitude is ~0.075 μm. Magnani et al.[53] presented a method on diode lasers including an electronic feedback loop for increasing the measurement resolution. This system is able to measure vibrations up to 110 mm peak-to-peak at a distance of 1 m, with bandwidth between 5 Hz and 15 kHz and resolution of about 60 nm. Wu et al.[54] constructed a single-channel laser feedback interferometer that measures the magnitude of the vibration and the angle of the position at the same time. The curve of the peak frequency versus the vibration amplitude follows the linear distribution, whereas the curve of the difference between the peak power versus the angle follows a Gaussian distribution. Lukashkin et al.[55] measured basilar membrane vibrations by laser feedback interferometer without opening the cochlea. Giuliani et al.[56] demonstrated a laser vibrometer based on the self-mixing interferometric effect in a laser diode. The system has features such as better than 100 pm Hz$^{-1/2}$ noise equivalent vibration, 180 μm peak-to-peak maximum measurable vibration, larger than 100-dB dynamic range, 70-kHz bandwidth, and successful operation on most rough surfaces. Huang et al.[57] proposed a vibration system extreme points model based on the laser feedback effect; the piezoelectric coefficient of a piezoelectric transducer in which d_{33} is 0.66034 nm/V was obtained. Chen et al.[58] investigated a simple damping microvibration measuring method that can accurately obtain the damping factor. The damping factor is solved by recording the period and counting the fringe number of the self-mixing signal. The damping factor of 0.0483 s^{-1} with a standard deviation of 0.0013 and the coefficient of variation of 2.69% were experimentally achieved.

3.3 Distance Measurement

Distance measurement with optical methods is widely used. However, the traditional methods have a distance measurement range limited by the power of the laser, and the accuracy is hard to ensure. Due to the high sensitivity in laser feedback interferometry and its simplicity in structure, which causes less loss to laser power, laser feedback interferometry is applied in the field of distance measurement. Shinohara et al.[59] put forward the method of distance measurement using a self-mixing laser diode. The interferometer measures the averaged mode hop time interval of successive external mode hops by the backscattered light from a target. The interferometer has precision of $\pm15\%$ in the wide range of 0.2 to 1 m. Since then, the laser feedback effect in diode lasers has been widely utilized for distance measurement.

Laser feedback interferometers based on laser diodes have a feature that a small variation in the laser driving current will produce an approximately linear variation in the laser operating frequency.[60] By utilizing this feature, a periodic modulation in the driving current will lead to frequency sweeping in the output of laser diodes. With the method of injected current reshaping in a laser self-mixing interferometer based on VCSEL proposed by Kou et al.,[61] a precise distance measurement can be achieved. A decrease in wavelength has a similar effect as a scattering object moving away from the laser source, whereas an increase in wavelength mimics an object moving toward the source. A sawtooth-shaped tuning current is utilized to drive the VCSEL to demonstrate the change of the beat frequency. The relationship between the laser wavelength and the frequency versus the injected current is researched. Each value of the divided frequency is used to deduce backward to the corresponding injected current, which eliminates the nonlinearity. Therefore, the injected current is reshaped. The reshaped injected current technique is effective for reducing the nonlinearity in current tuning, and the resolution of the distance measurement is improved to be 20 μm in the range from 2.4 to 20.4 cm.

Moench et al.,[62] Michalzik,[63] and Gouaux et al.[64] also applied the VCSEL laser feedback interferometer based on the modulation of the working current. Guo et al.[65] proposed a method based on a double-modulation technique on a laser diode for absolute distance measurement. The intensity of the laser and the amplitude of phase are both modulated to raise the resolution. The absolute distance has been measured with a resolution of ±0.3 mm over the range of 277 to 477 mm.

3.4 Velocity Measurement

Velocity measurement is another important field in metrology. Velocity is usually measured by the laser Doppler velocimeter employing the Doppler effect. Since 1968, when Rudd[66] applied the laser feedback effect in velocity measurement, laser feedback velocimeters have been the research foci.[67,68] The signal curve of the velocimeter is in sawtooth shape and the discrimination of the movement directions is researched.[69,70] In the laser feedback field, the laser feedback Doppler velocimeter is a type of compact and high cost-effective Doppler velocimeter with high precision.

One of the most attractive velocimeters uses the three perpendicular beams fiber irradiation scheme. Initially, Mikami and Fujikawa[71] proposed a two-beam irradiation

scheme. In the two-beam irradiation structure, the two beams are irradiated at one spot on the target. The offset angle between the two beams is set to be $\Delta\theta$. In this configuration, the interference takes place and the Doppler shift frequencies can be obtained by the spectrum analyzer. Then, the velocity of the target V can be expressed as follows:

$$V = \frac{\lambda}{2\sin\Delta\theta}\sqrt{f_1^2 + f_2^2 - 2f_1 f_2 \cos\Delta\theta}. \tag{25}$$

It can be seen that the velocity of the target can be obtained only with prior knowledge of the offset $\Delta\theta$. However, the two-beam scheme demands that the velocity vector of the target is on the same plane with two irradiation beams. To solve the issue in the two-beam velocimeter, the three-beam scheme is proposed. The beam from a laser diode having a single longitudinal mode is divided into three beams by the fiber couplers. The three irradiation beams of the sensor head are set perpendicular to one another. Therefore, each beam direction is considered the axis of the orthogonal coordinate system. The configuration and experimental setup are shown in Fig. 6. By this method, the measurement of arbitrary velocity can be fulfilled.

Scalise et al.[72] developed a new model and a suitable processing algorithm for the analysis of the signal in the case of relevant speckle effects. Bosch et al.[73] employed multimode VCSELs for velocity measurements, which can be of great interest due to its low price, high stability, and low threshold. In the applications of the laser feedback velocimeters, the scattering of the laser emission from a rough surface will lead to a speckle effect that models the Doppler signal, causing broadening of the signal spectrum and adding uncertainty to the velocity measurement. To eliminate this uncertainty induced by the speckle effect, various research has been done and different methods, such as analytic equation prediction[74] and fractal analysis with box-counting,[75] are employed. Huang et al.[76] studied the results of the speckle self-mixing velocimeter concerning the angles of incidence. The relative error drops dramatically with the incident angle increasing from 5 to 30 deg. Özdemir et al.[77] proposed the autocorrelation data processing method for speckle self-mixing velocimeter; effects of various parameters have been analyzed and the system has been optimized with fewer measurement errors. The linear relation between the reciprocal of the autocorrelation time of the speckle signal obtained and the velocity of the target has been analyzed.[78] By

employing another laser diode, simultaneous measurement of velocity and length of moving targets with homogeneous rough plane surfaces can be realized.[79] Shinohara et al.[80] have also applied the speckle effect of the self-mixing interferometer for surface classification, making the method inexpensive and highly sensitive.

In addition to the measurement of the velocities in solid targets, the velocity of flowing liquid can also be measured by applying a laser diode self-mixing technique.[81] Compared with the traditional method using microparticle imaging velocimetry, which has disadvantages such as being complex, time-consuming, and bulky, laser feedback interferometry has a simpler structure and faster response in flow measurement. Fluid velocity measurements of water seeded with titanium dioxide have been performed using a diode to measure the effect of the seeding particle concentration and the pump speed of the flow. The laser light was focused at the center of the fluid discharging from the nozzle. The measured velocity linearly increases with the pump speed as expected. The system has demonstrated accuracy better than 10% for liquid flow velocities up to 1.5 m/s with a concentration of scattering particles in the range of 0.8% to 0.03%. By using different types of seeders, higher velocity measurement can be realized. Campagnolo et al.[82] reported the work of flow profile measurement in microchannels applying a VCSEL laser feedback interferometer. In this work, the measurement of local velocity in fluids with spatial resolution in the micrometer range is achieved by minimizing the laser spot size with the diameter being 32.26 μm. Ramírez-Miquet et al.[83] utilized a blue–violet laser diode with a wavelength of 405 nm, which is capable of measuring very slow velocities. The system is found to be a good representation of the liquid–liquid two-phase system's hydrodynamics.

With the growing need for accurate diagnosis and disease prevention in biology and the medical fields, precise measurement of blood flow in vessels and tissues is attracting greater research attention. The invasive measurement of skin, capillary, or cutaneous blood flow is considered to be significant and can be used for the assessment of vasopasm, ischemia, wound and ulcer healing, skin diseases, therapeutic trials, and various pathological conditions.[84] A very active research focus in this field is laser feedback interferometry. Since de Mul et al.,[85] Slot et al.,[86] and Mito et al.[87] first utilized the self-mixing Doppler phenomenon for blood
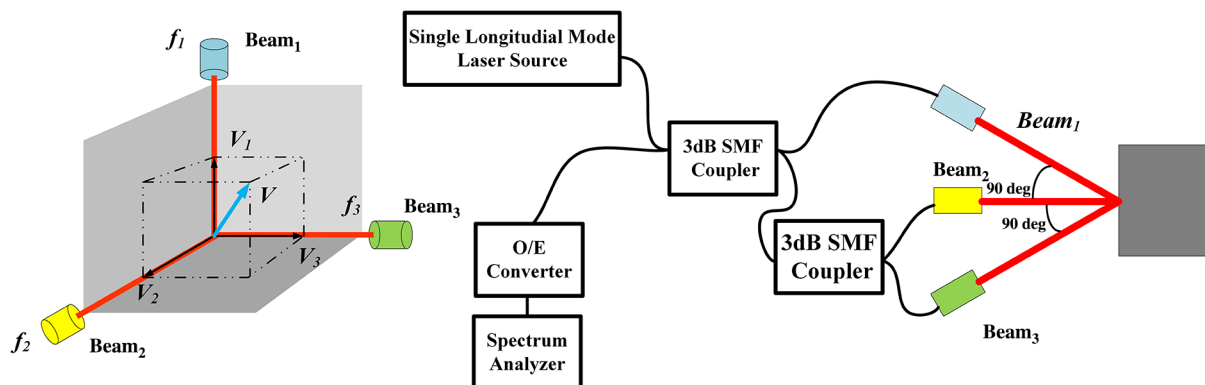

Fig. 6 Configuration and experimental setup of the three-beam self-mixing velocimeter. f, frequency of the beam; V, velocity of the target.
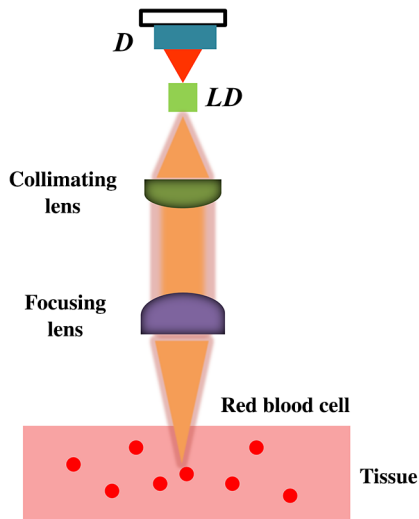
Fig. 7 Experimental setup of laser self-mixing velocimeter for flow measurement. D, detector; LD, laser diode.

flow measurements, multiple studies have been done on this subject. Shinohara et al.[88,89] utilized the self-mixing speckle signal of backscattered light from the red blood cells and the speckle autocorrelation method to realize blood flow measurement. The experimental setup is shown in Fig. 7. The system has the capability of measuring blood flow at speeds from 30 to 125 mm/s. Norgia et al.[90] applied the fast Fourier transformation method and logarithm-weighted mean to optimize the linearity of the system. The accuracy was better than 0.1 L/min in the large range of 0 to 6 L/min of clinical interest. Figueiras et al.[91] applied the laser self-mixing velocimeter as a microprobe for monitoring microvascular perfusion in rat brain. The mean detection depth was 0.15 mm, and the size of the probe was as small as 785 nm. The authors also introduced three signal processing methods, including the counting method, autocorrelation method and power spectrum method, which supplied efficient methods for data processing.

In addition, Zhao et al.[92] presented a method of velocity measurement using a self-mixing velocimeter with an orthogonal beam incident system, which enables velocity measurement without knowing the incident angle information. The fiber ring laser acts as a stable and narrow-width laser light source, which could enhance the stability and the signal-to-noise ratio of the self-mixing fiber ring laser velocimeter. The relative error rates of this velocimeter system are up to 1.258%.

3.5 Angle Measurement

The noncontact precise measurement of angles is strongly needed in industrial and research situations. The traditional methods, such as autocollimator or laser interferometers, usually need a reflective mirror, which limits the application. Since the laser feedback effect has high sensitivity, it can be applied in adjusting the remote mirror or angle measurement.[93] One solution to precise angle measurement proposed by Zhang et al.[94] is the parallel multiplex laser feedback interferometer. The system setup is similar to Fig. 3; however, the laser in the parallel multiplex laser feedback interferometer is produced by two parallel laser diodes pumping

one microchip. The system also applies frequency-shifted feedback interferometry. From the configuration, it can be seen that the laser emits two parallel beams at different positions on the same target. The displacements of these positions are measured at the same time. Therefore, the displacement difference reflects the angle variation of the target. This scheme does not generate any signal crosstalk for several reasons. First, only when the laser beams go back exactly along the same path injecting to the target can the frequency of the beam be shifted by 2Ω and demodulated by the heterodyne phase measurement, which effectively restrains the external noise. Second, although the two beams are generated in the same microchip, the frequencies of the beams are different from each other. Thus, there is no cross interference. The beat frequency of the two beams can be filtered. Third, the two optical paths are very close, so the displacement difference, which is the subtraction of the two measured displacements, can eliminate the environmental disturbance and thus accurately reflect the angle variation. The measurement results are compared with the laser interferometer Agilent 5529A. The parallel multiplex laser feedback interferometer exhibits good stability with the maximum nonlinear error of 8″ in the range of 1400″.

Another method for angle measurement is applying the external-cavity birefringence feedback effects of a microchip laser proposed by Ren et al.[95] The wave plate inside the external feedback cavity has the role of producing the external-cavity birefringence feedback. The cross-section of the refractive index ellipsoid of the wave plate is an ellipse. It can be seen that, based on the external birefringence feedback, the information of the roll angle in the birefringence element placed inside the external cavity can be transferred into the phase difference between the two orthogonally polarized beams. Giuliani et al.[96] proposed a technique to measure the angle of a remote flat surface with respect to the propagation direction of the laser beam, based on injection detection in a laser diode. The technique enables the measurement of angles with a sensitivity of 5×10^{-7} rad. Zhong et al.[97] presented a signal defining method that places the refractive mirror on the surface of the object for measuring a small angle. The rotation angles are measured with an accuracy of 10^{-6} rad. The angle measurement range is approximately -0.0007 to $+0.0007$ rad. As mentioned above in Ref. 53, the simultaneous measurement of vibration and the angle of the position of the target relative to the incident beam can be realized. The rotation angle over a range of 0.075 deg can be measured, with the error <11.7%. Tan and Zhang[98] also proposed a system including two orthogonally linearly polarized modes produced by a tunable frequency difference that exists in microchip lasers with two quarter-wave plates in the laser inner cavity. The frequency difference relates to the orientation of one quarter-wave plate. The sensitivity can be as high as 0.3 arc sec, which is 1.6×10^{-6} rad.

3.6 Thickness Measurement

Precise measurement of the thickness of optical elements plays a significant role in optical industrial applications. However, there is a lack of effective testing methods other than contacting methods, which have low accuracy and cause damage to the optical elements. The laser feedback effect has been applied in thickness measurement by Fathi
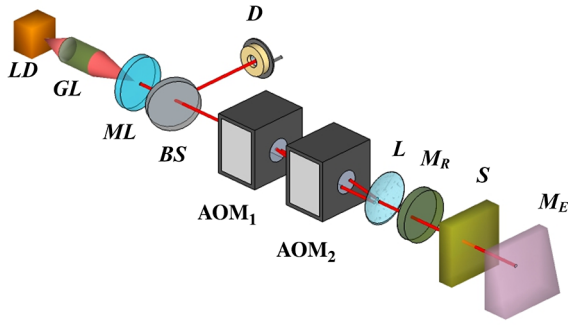
Fig. 8 Configuration of frequency shift feedback thickness measurement system. LD, laser diode; GL, grin lens; ML, microchip laser; BS, beam splitter; D, detector; AOM, acousto-optic modulators; L, lens; M_R, reference mirror; S, sample; M_E, optical wedge as the measurement mirror.

and Donati[99] Considering the high sensitivity of frequency shift feedback, the frequency-shifted laser feedback interferometer has been used for thickness measurement.[100] The configuration is shown in Fig. 8.

By rotating the sample inserted into the external feedback cavity, the optical path difference induced can be measured by the laser feedback interferometer. The optical path change in the rotating sample can be derived as

$$\Delta L = (\Delta \varphi_m - \Delta \varphi_r) \frac{\lambda}{2\pi}$$
$$= d \left(\begin{array}{c} \sqrt{n^2 - n_0^2 \sin^2 \theta_2} - n_0 \cos \theta_2 \\ -\sqrt{n^2 - n_0^2 \sin^2 \theta_1} + n_0 \cos \theta_1 \end{array} \right), \quad (26)$$

where ΔL denotes the optical path change induced by the rotation of the sample, λ is the laser wavelength, d is the thickness of the sample, n is the refractive index of the sample, n_0 is the refractive index of the air, and θ_1 and θ_2 are the angles between the laser beam and the normal direction of the sample surface before and after the rotation. By measuring θ_2 and ΔL at multiple angles, the overdetermined equation can be solved and the thickness of the sample can be obtained together with the refractive index. Through the experiments, the measurement uncertainty of the thickness is better than 0.0006 mm. However, in measuring the thickness, this method requires the sample to be flat and parallel. The parallelism is better than 2″ in the reference. Due to the fact that the sample needs to be rotated, if the sample is not parallel or flat, after the rotation, the thickness d in Eq. (26) is hard to maintain, which causes a large error in measurement. Also, the measurement procedure needs to be combined with the rotation of the sample at high precision angles. Another method proposed by Tan et al.[101,102] combining the confocal effect and frequency shift feedback, which is noncontact, nondestruction, and highly sensitive, can be applied in measurement not only of the thickness but also between the air gap. The schematic setup of the system is shown in Fig. 9.

The laser is separated into two beams by the beam splitter. The measuring light selected is expanded and collimated via the beam expander. The annular pupil is inserted into the path before the objective lens to create the annual beam. There exists a conjugation relationship between the focus point of the objective lens and the laser beam waist. The light intensity modulation under the confocal effect is expressed as
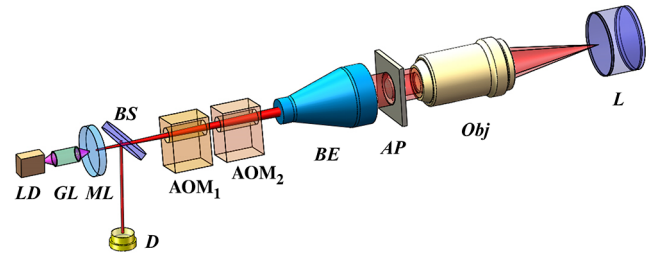

Fig. 9 Schematic diagram of the laser frequency shifted confocal system. LD, laser diode; GL, grin lens; ML, microchip laser; BS, beam splitter; D, detector; AOM, acousto-optic modulators; BE, beam expander; AP, annular pupil; Obj, objective lens.

$$I(u) = \left| \frac{\sin[(1 - \varepsilon^2)u/2]}{(1 - \varepsilon^2)u/2} \right|^2, \qquad u = \frac{8\pi}{\lambda} z \sin^2(\alpha/2), \quad (27)$$

where z is the defocus distance, α is the numerical aperture angle of the object lens, and ε is the ratio of the inner and outer diameters caused by the annular pupil. The intensity modulation in the frequency-shifted confocal feedback can be derived as follows:

$$\frac{\Delta I(2\Omega)}{I_s} = \left| \frac{\sin[(1 - \varepsilon^2)u/2]}{(1 - \varepsilon^2)u/2} \right|^2 \cdot \kappa G(2\Omega) \cos(2\Omega t - \phi + \phi_s). \quad (28)$$

The simulation and experimental results are shown in the Figs. 10(a) and 10(b).

The lens thickness and the air gap between the lenses are measured in the experiments. The system has an uncertainty of axial positioning better than 0.0005 mm, and the accuracy is on the order of microns. The system has the potential to be implemented for the measurement of lenses coated with multilayer films.

Above are six typical aspects of applications of laser feedback interferometry in the fields of metrology; although there exist many other applications in metrology, the most common methods are explained in detail and provide an introduction for the metrological application.

4 Laser Feedback Technology Applications in Laser Parameters Measurement

It has been known that laser feedback interferometers have the capability to detect changes in the external feedback cavity and information in the target. However, it can be seen during research on the laser feedback effect that the laser feedback waveforms are closely related to the parameters of the lasers. Therefore, the measurement of laser parameters by the laser feedback effect is studied deeply. The laser linewidth, linewidth enhancement factor, and laser polarization cross-saturation coefficient of semiconductor and solid-state lasers are important parameters in laser technology. Precise measurements of these parameters provide significant guidance in laser application fields.

4.1 Laser Linewidth Measurement

In the laser feedback field, the laser feedback signal waveforms in the laser diodes are related to the physical parameters of the laser sources. The linewidth can be evaluated from the phase noise in the feedback waveforms. The
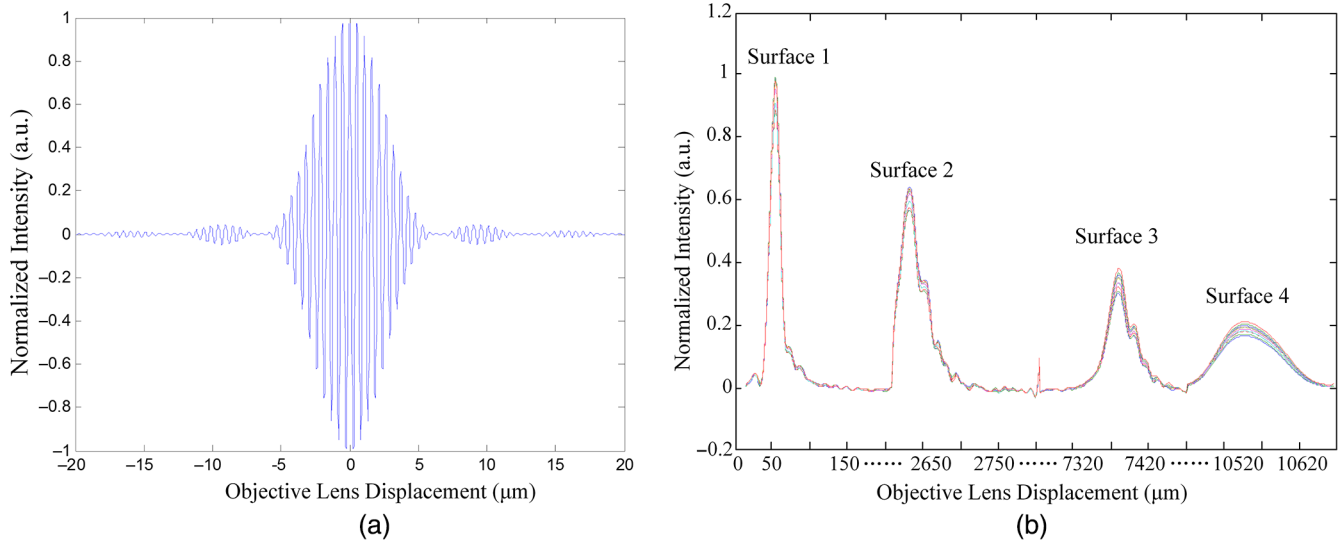
Fig. 10 Results of laser frequency-shifted confocal feedback system. (a) Simulation results and (b) measured results.

sawtooth shape of self-mixing interferometry is the key point for the accurate measurement of the phase noise, which can be applied for linewidth measurement.[103] The method has advantages such as simplicity, self-alignment, and no need for frequency measurement. When the feedback level is set at a certain value, the laser feedback waveform can be modulated in a sawtooth shape when the measured target has movement driven by a sinusoidal wave.

When the light is reinjected into the laser cavity, phase noise will be generated by the fluctuation of the laser frequency and by the target distance fluctuation. Suppose the frequency of the laser diode is $\nu = \nu_0 + \Delta\nu$, where $\Delta\nu$ is the fluctuation of the frequency, and the distance of the target is $D = D_0 + \Delta D + D(t)$, where $D(t)$ is the sinusoidal displacement and ΔD is the fluctuation of the distance. Then, the phase noise can be derived as follows:

$$\sqrt{\langle\Delta\phi^2\rangle} = \frac{4\pi}{c}\sqrt{\nu_o^2\langle\Delta D^2\rangle + D_o^2\langle\Delta\nu^2\rangle}. \tag{29}$$

When the phase noise is measured as a function of the target distance, with the condition that $\nu_o^2\langle\Delta D^2\rangle \ll D_o^2\langle\Delta\nu^2\rangle$, a linear dependence of the phase noise can be set as follows:

$$\sqrt{\langle\Delta\phi^2\rangle} = \frac{4\pi D_o}{c}\sqrt{\langle\Delta\nu^2\rangle}. \tag{30}$$

From the slope in the linear function, the linewidth of the laser diode can be easily determined by the method of laser feedback effect.

4.2 Linewidth Enhancement Factor Measurement

The linewidth enhancement factor α is a fundamental parameter in semiconductor lasers.[104] Semiconductor lasers exhibit a strong variation of refractive index and gain when the injected carrier density is changed. It is a comprehensive parameter of the laser linewidth, the chirp, the injection lock range, and the response of the laser feedback.[105] The linewidth enhancement factor determines the dynamics of semiconductor lasers since it accounts for the coupling between amplitudes and phases of the laser. The linewidth enhancement factor α can be expressed as[106]

$$\alpha = -\frac{\partial x'/\partial N}{\partial x''/\partial N} = -\frac{4\pi}{\lambda}\cdot\frac{\partial\eta/\partial N}{\partial g/\partial N}, \tag{31}$$

where x' and x'' are the real and imaginary parts of the susceptibility of the laser active medium, N is the carrier density, η is the refractive index, and g is the optical gain. As a result, the linewidth enhancement factor α is responsible for the linewidth enhancement and affects the modulation response, frequency chirping, injection locking ranges, and stability of lasers with external optical feedback. Therefore, precise measurement of the linewidth enhancement factor α is of great significance in the fields of semiconductor lasers and self-mixing interferometers based on semiconductor lasers. One of the techniques to estimate the linewidth enhancement factor α is the genetic algorithm approach proposed by Wei et al.[107] With the Lang–Kobayashi model, the gain of the laser under the feedback effect can be seen as the function of the laser phase, the backreflected laser phase, and the laser linewidth enhancement factor. Suppose the target is having a simple vibration $L(t) = L_0 + \Delta L\cos(2\pi ft + \theta_0)$, then the value of the feedback signal can be expressed as

$$G(t) = \cos\left[\begin{array}{c}\varphi_0 + \Delta\varphi\cos(2\pi ft + \theta_0)\\ -C\sin\{\phi_F[\tau(t)] + \arctan(\alpha)\}\end{array}\right], \tag{32}$$

where φ_0 and $\Delta\varphi$ are the phases of the backreflected light, ϕ_F is the laser phase under the feedback effect, and C is the feedback level. The unknown four parameters are φ_0, $\Delta\varphi$, C, and α. The minimization of the cost function can be expressed as

$$F(\widehat{\varphi_0}, \widehat{\Delta\varphi}, \hat{C}, \hat{\alpha}) = \frac{1}{N}\sum_{i=1}^{N}[G_i - \hat{G}_i(\widehat{\varphi_0}, \widehat{\Delta\varphi}, \hat{C}, \hat{\alpha})]^2, \tag{33}$$

where G_i is the measured signal value and $\widehat{G_i}$ is the theoretical calculated value. By the genetic algorithm approach,

the parameter of semiconductor lasers can be determined. von Staden et al.[108] reported the method for linewidth enhancement factor measurement in QCLs. The method applies the time interval detected in the feedback signal curve. Yu et al.[109] proposed the automatic method using the self-mixing signal under weak optical feedback. The method does not need to foreknow the exact movement of the target, and it has robustness and noise immunization, with a standard deviation <4.58%.

In addition, Szwaj et al.[110] proposed the method based on variations of the laser relaxation frequency when the laser is subjected to an optical feedback. This method consists of measuring the phase shift between the variation of the relaxation frequency and the variation of the output intensity when the laser is subjected to a modulated round-trip time feedback. In the case of large feedback, the effect of α is directly observable on the laser average intensity.

The linewidth enhancement factor α can characterize the response of lasers to external feedback; as a result, the precise measurement of α is crucial in determining the performance of lasers under the laser feedback effect.

4.3 *Laser Polarization Cross Saturation Coefficient Measurement*

In the research of orthogonally polarized light feedback, unlike the single polarization feedback, the initial gain of the laser can be divided into two parts corresponding to the intrinsic orthogonal polarization direction of the laser. These two parts of the gain can be connected by the cross-saturation coefficient β and the rate equations of orthogonally polarized lights.[111] The rate equations are divided as the vertical polarization eigenstate system $(N_\perp, I_\perp)$ and the parallel polarization eigenstate system $(N_\parallel, I_\parallel)$. The rate equations coupled by the two orthogonal polarizations in the laser can be expressed as[112]

$$\begin{cases} \frac{dN_\perp}{dt} = \gamma_1[w - (1 + I_\perp + \beta I_\parallel)N_\perp] \\ \frac{dN_\parallel}{dt} = \gamma_1[w - (1 + I_\parallel + \beta I_\perp)N_\parallel] \\ \frac{dI_\perp}{dt} = \gamma_c(N_\perp + \beta N_\parallel - 1)I_\perp \\ \frac{dI_\parallel}{dt} = \gamma_c(N_\parallel + \beta N_\perp - 1)I_\parallel \end{cases}, \quad (34)$$

where N is the population inversion, I is the laser intensity, γ_1 is the inversion particle population decay rate, γ_c is the photon population decay rate, w is the normalized pumping parameter, and β is the cross saturation coefficient describing how each laser field is coupled with the population inversion of the other laser subsystem.

Suppose the angular frequency of the two orthogonally polarized lights is ϕ_i, κ is the effective reflectivity. Make $\kappa_\parallel = 0$, under the condition of weak feedback, the laser intensities can be derived as follows:

$$\begin{cases} I_\perp^s + I_\parallel^s \approx \frac{-2}{1+\beta} + 2w + 2w\kappa_\perp \cos \phi_\perp \\ I_\perp^s - I_\parallel^s \approx \frac{w(1+\beta)^2}{(1-\beta)^2} + \frac{(1+\beta)^2}{(1-\beta)^2} 2w\kappa_\perp \cos \phi_\perp \end{cases}. \quad (35)$$

The variation in the sum and difference of the intensities of the polarization states can be derived as follows:

$$\begin{cases} \Delta I_+ = \Delta(I_\perp^s + I_\parallel^s) = 2w\kappa_\perp \cos \phi_\perp \\ \Delta I_- = \Delta(I_\perp^s - I_\parallel^s) = \frac{(1+\beta)^2}{(1-\beta)^2} 2w\kappa_\perp \cos \phi_\perp \end{cases}. \quad (36)$$

Then, the cross-saturation coefficient β can be derived as follows:

$$\beta = \frac{\sqrt{\Delta I_-/\Delta I_+} - 1}{\sqrt{\Delta I_-/\Delta I_+} + 1}. \quad (37)$$

The method has advantages such as convenience and no demand for the pumping level, which can be carried out easily.

Using the laser feedback effect for laser parameters measurement has advantages such as simple alignment and high precision. The results are in good coincidence with the theoretical analyses. The above techniques provide reliable choices for laser parameters measurement in both semiconductor lasers and solid-state lasers with fewer optical components and fewer devices.

5 Laser Feedback Technology Applications in Physical Quantities Measurement

A physical quantity (or physical magnitude) is a physical property of a phenomenon, body, or substance that can be quantified by measurement. Although the physical quantities cannot be measured directly, they can be calculated by employing the measurement in metrology. The physical quantities such as refractive index, birefringence, evaporation rate of the liquid, and thermal expansion index are important parameters in the fields of materials. Imaging of acoustic fields distribution is of importance for acoustic detection. By applying laser feedback interferometry, the measurements of the physical quantities are shown as follows.

5.1 *Refractive Index Measurement*

In optics, the refractive index or index of refraction n of a material is a dimensionless number that describes how light propagates through that medium. The refractive index is a very important property of the components of any optical instrument that involves refraction. It determines the focusing power of lenses, the dispersive power of prisms, and, generally, the path of light through the system. As mentioned above in Sec. 3.6, the method of rotating a transparent parallel sample in the laser frequency shift feedback system can be applied in the simultaneous measurement of thickness and refractive index. The refractive indices of three different kinds of materials—including calcium fluoride (CaF_2), fused silica, and zinc selenide (ZnSe)—are measured in the system.[113] The refractive indices cover a large range from 1.42874 to 2.48272. The experiment shows that the measurement uncertainty of the refractive index is better than 0.00003. The method has advantages such as high precision, wide measuring range, easy data processing, and environmental robustness.

The refractive indices of solid samples can be easily obtained by the above method. However, when it comes to the refractive indices of liquids, since the sample cannot be rotated, the method has to be adjusted. Utilizing the high sensitivity of the frequency shift feedback effect, a double-beam laser frequency shift feedback interferometer is

proposed for measuring the refractive indices of liquids by Xu et al.[114]

When the liquid level increases Δh, the changes of the external cavity lengths in the two beams are as follows:

$$\begin{cases} \Delta L_1 = -n_0 \times \Delta h \\ \Delta L_2 = (n - n_0) \times \Delta h \end{cases}, \tag{38}$$

where n_o is the air refractive index and n is the liquid refractive index to be measured, which can be expressed as follows:

$$n = n_0 \times \left(1 - \frac{\Delta L_2}{\Delta L_1}\right). \tag{39}$$

The calculation of the refractive index depends entirely on the changes of the external cavity length as well as the air refractive index and is not related to the parameters of the container. The particle deviations of Eq. (39) are as follows:

$$\begin{cases} \frac{\partial n}{\partial(\Delta L_1)} = n_0 \frac{\Delta L_2}{\Delta L_1^2} = \frac{n - n_0}{n_0 \times \Delta h} \\ \frac{\partial n}{\partial(\Delta L_2)} = -n_0 \frac{1}{\Delta L_1} = \frac{1}{\Delta h} \end{cases}. \tag{40}$$

Since the resolution of the laser frequency shift feedback interferometer is 1 nm, considering the environmental disturbance, the effective resolution of the refractive index can reach 10^{-6}. The refractive indices of the distilled water, ethanol, cyclohexane, silicone oil, and engine oil are measured. Through experiments and theoretical analysis, the system has high repeatability, which is better than 0.00005.
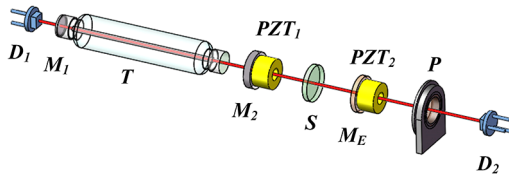

Fig. 11 Experimental setup of polarization flipping with hysteresis. D, detectors; M1, M2, laser cavity mirrors; T, laser tube; S, sample; P, polarizer; M_E, feedback mirror; PZT, piezoelectric transducer.

5.2 Birefringence Measurement

Birefringence is the optical property of a material having a refractive index that depends on the polarization and propagation direction of light. As a significant parameter in the optical system, birefringence has a great impact on the optical properties and performances. On one hand, birefringent elements, such as wave plates and quartz crystals, have functions such as modulating the phase properties in the optical systems; on the other hand, the unexpected birefringence such as the inhomogeneous stress-induced birefringence will bring harmful effects upon systems demanding the polarization-preserving property. As a result, the precise measurement of birefringence is of great significance.

The polarization dynamics of a laser subjected to weak optical feedback from the birefringence external cavity are studied theoretically and experimentally by Fei et al.[115] It is found that polarization flipping with hysteresis is induced by birefringence feedback, and the intensities of two eigenstates are both modulated by the external cavity length. The variations of hysteresis loop and duty ratios of two eigenstates in one period of intensity modulation are related to the phase differences of the birefringence element in the external cavity. The relationship between the polarization flipping and the birefringence in the external cavity is studied by Chen et al.[116] The experimental setup is shown in Fig. 11.

A piezoelectric transducer (PZT) is controlled by a periodical triangular-wave voltage and drives M_E to do the reciprocating movement in order to modulate the length of the external cavity. As analyzed in the three-mirror model, the intensity of the laser is proportional to the equivalent reflectivity; when the length of the external cavity is changed by the reciprocating movement of the feedback mirror, the intensity of the laser is modulated cosinoidally, as shown in Fig. 12(a). When the birefringence element is inserted into the laser external feedback cavity, suppose the phase shift caused by the birefringence is δ. Then, the equivalent reflectivity of the two polarizations in the laser feedback system can be expressed as follows:[117]

$$R_{\text{eff}}^o = R_2 + 2R_2^{1/2}(1 - R_2)(1 - R_E)^{1/2} \cos(2Kl),$$

$$R_{\text{eff}}^E = R_2 + 2R_2^{1/2}(1 - R_2)(1 - R_E)^{1/2} \cos(2Kl + 2\delta). \tag{41}$$
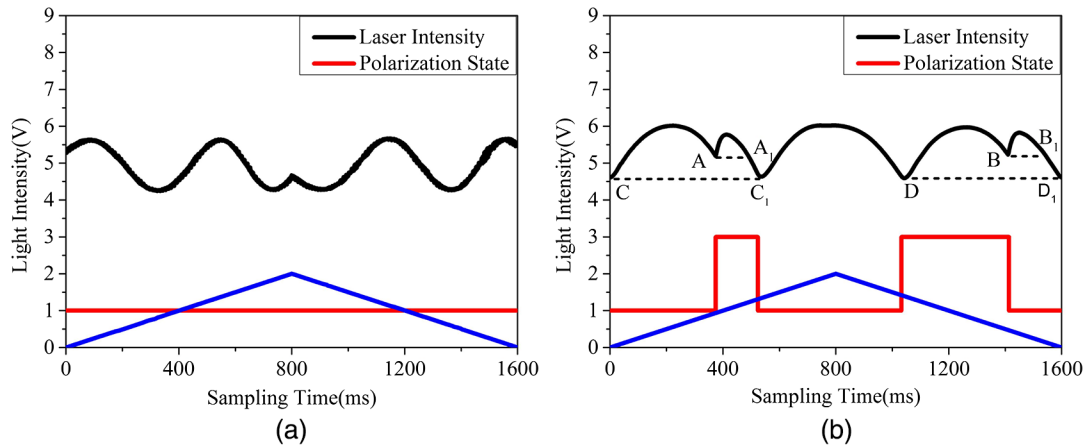

Fig. 12 Experimental curves of laser feedback and polarization flipping in laser feedback system. (a) The birefringent sample is not inserted in the external cavity. (b) The sample is inserted in the external cavity. A, B, polarization flipping points; A_1, B_1, corresponding isocandela points; C, C_1, D, D_1, tuning period points.

Since there are two polarization states, when the periodical triangular-wave voltage drives the movement of PZT and M_E, the length of the external cavity and the equivalent reflectivity of the two polarizations are tuned. Mode competition between the two polarizations will occur. The different modes correspond to two different equivalent reflectivities. When one equivalent reflectivity is higher, the cavity loss is less. Consequently, the corresponding mode will have superiority in mode competition. The polarization state of the beam is induced by the result of mode competition. As a result, there will be a mutation in laser intensity and a flipping in the polarization state of the beam.

In the increasing region of PZT driving voltage, the polarization flipping point in the laser intensity curve is A and its corresponding isocandela point is A_1. The tuning period is from C to C_1. The same goes to the decreasing region with B, B_1, D, and D_1. According to Eq. (41), the phase shift δ can be deduced as follows:

$$\delta = \frac{1}{2} \times \left(\frac{l_{AA_1}}{l_{CC_1}} + \frac{l_{BB_1}}{l_{DD_1}} \right) \times 180 \ \text{deg}. \tag{42}$$

The system has advantages, such as high precision and robustness to environmental disturbance, which can fulfill online measurement of the birefringence. The measurement accuracy of the birefringence is <0.22 deg.[118]

In the manufacturing process of the optical elements, the inhomogenity of temperature or the external disturbance will cause internal stress in elements. The stress-induced birefringence inside the optical elements such as lenses and mirrors will cause damage to the phase prosperity of the optical system, and stress in glasses, particularly in specific situations such as in aircraft, may cause accidents due to cracking. Therefore, precise measurement of this stress offers great benefits and significant guidance to optical systems and industrial applications. The optical path difference Δl_o in the center of the optical element is

$$\Delta l_o = \frac{8\lambda}{\pi D f_0} \cdot F, \tag{43}$$

where λ is the wavelength of the laser, D is the diameter of the optical element, f_0 is the material fringe value, and F is

the value of the stress. The stress of the optical elements is linearly related to the birefringence. As a result, the internal stress can be measured precisely as well.[119]

5.3 Thermal Expansion Coefficient Measurement

The thermal expansion coefficient describes how the size of an object changes with a change in temperature. The thermal expansion coefficient is one of the most fundamental quantities of materials, which is intrinsically related to other thermophysical properties. Accurate measurement of the thermal expansion coefficient is of significance in basic scientific research and industrial applications. However, in previous methods, noncontact methods demand a specific range of measurable materials and a limited working temperature range while the measurement process suffers environmental disturbances. The whole measuring beam path belongs to the dead path, making it difficult to increase accuracy and repeatability. A method based on the microchip frequency shift feedback interferometer with compensation by the quasi common path structure is proposed by Zheng et al.[120] The influence of distortion in the sample supporter is compensated by the symmetric structures, where the measurement beams of two symmetric laser feedback interferometers inject perpendicularly and coaxially on opposite surfaces of the sample. The schematic diagram of the measuring system is shown in Fig. 13.

The positions of the two systems are adjusted to make the beams cross the furnace, and in particular, the two measurement beams are adjusted to ensure that they are in a single line so the Abbe error can be reduced as much as possible. The measurement repeatability of thermal expansion coefficients is better than $0.6 \times 10^{-6} \ (\text{K}^{-1})$ at the range of 298 to 598 K. The system has realized highly sensitive noncontact measurement of the low reflectivity surface induced by the oxidization of the samples at 598 to 748 K.[121] Therefore, with the advantages of being noncooperative and highly sensitive, this study is of great significance to the study of high precision thermal expansion coefficient determination of materials at a wide temperature range.[122]
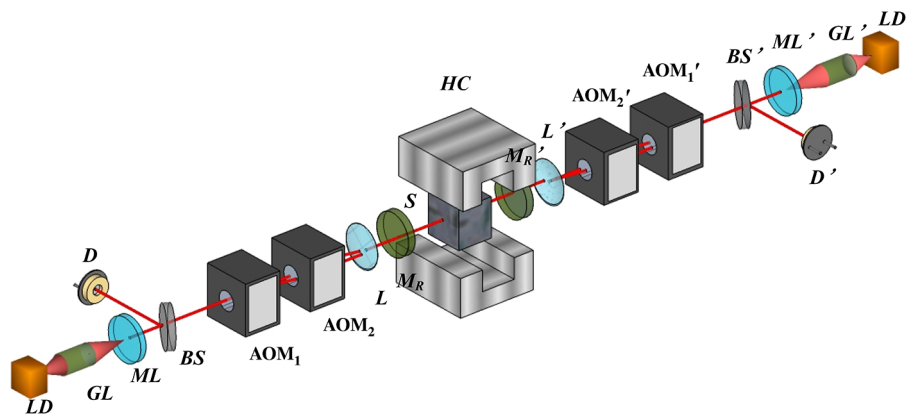

Fig. 13 Schematic diagram of the measurement of thermal expansion coefficient based on the microchip laser feedback interferometers. LD, LD′, laser diodes; ML, ML′, microchip lasers; BS, BS′, beam splitters; D, D′, detectors; AOM, AOM′, acousto-optic modulators; L, L′, lenses; M_R, M'_R, reference mirror; HC, heating cabinet.

5.4 Evaporation Rate of Liquid and Liquid Level Measurement

Liquid level measurement is fundamental in many industrial occasions. The ordinary methods, including mechanical and pressure-based sensors, are contact-based and limited to certain kinds of liquids. Yet the real-time measurement and accuracy need to be improved. The laser feedback interferometer can also be applied in liquid level measurement.[123] The laser used is a laser diode in which the driving current is in the form of a triangular wave. The appearance of the liquid surface can be divided into two categories: the still surface and the choppy surface. In the still surface, the liquid is motionless, and the surface is flat. It can be assumed that its optical performance is similar to a mirror, and the beam is reflected in a coherent manner. In the choppy surface, the liquid is shaking at a relatively high frequency. The optical performance is similar to the target with a rough surface. In this case, instead of being reflected, a portion of the incident light is scattered in different directions. The two surfaces are optically different. The first one can induce laser instability when the reflected beam is perfectly redirected in the cavity, but it is extremely sensitive to deviation from the perpendicular condition between the laser and the liquid surface. In the second scenario, the optical power is spread due to the diffusion of the choppy surface. Therefore, there is always a possibility of reading a signal, even if it is not perpendicular to the water surface, but the amplitude could be very low.[124]

The volatility or evaporation rate of the liquid is another significant parameter, which is defined as the liquid level variation within a unit of time. When adjusting the beam incident perpendicularly into the liquid surface, the laser frequency shift feedback interferometer can be utilized for evaporation measurement.[125] On the basis of the structure of the frequency shift feedback interferometer, a hollow arm is installed at the interface of the interferometer, and the laser beam is turned by 90 deg with a right-angled prism fixed at the end of the hollow arm. The evaporation rates of four colorless transparent liquid samples, including distilled water, absolute alcohol with a proportion larger than 99.7%, acetone, and ether, are measured in the system. The evaporation rate of distilled water is 34 nm/s; alcohol is 172 nm/s, which is 5 times of that of water; acetone is 932 nm/s, which is 4 times greater than that of alcohol; and ether is 2349 nm/s, which is 3 times that of acetone, 14 times that of alcohol, and 2 orders higher than that of water.

5.5 Acoustic Fields Distribution Measurement

The visualization of sound field propagation in gases, fluids, and transparent media is of major interest in recent research. The traditional methods remain bulky and highly sensitive to mechanical perturbations, which limit the accuracy of measurement. Gamidov et al.[126] proposed a method for sound pressure measurement in a small volume based on optical feedback in single-mode diode laser. Based on this foundation, an ultra-simplified laser feedback interferometer system is designed to facilitate the direct sensing of the acoustic fields, permitting its reconstruction as 2-D images proposed by Bertling et al.[127] The schematic diagram is shown in Fig. 14.

According to the theoretical analyses above, the power output of the laser subject to optical feedback can be derived as
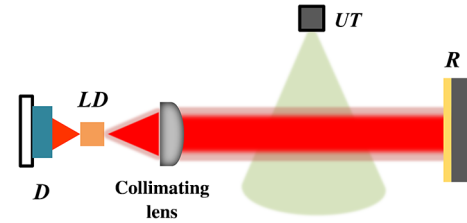

Fig. 14 Schematic diagram of the acoustic field measurement laser feedback interferometer. D, detector; LD, laser diode; UT, ultrasonic transducer; R, reflector.

$$P_F = P_0[1 + m \cos(\omega_F \tau)], \quad (44)$$

where P_0 is the power emitted by the stand-alone laser; m is the modulation index, which is strongly dependent on the external cavity length and the external cavity reflectivity; ω_F is the laser frequency under feedback; and τ is the external cavity round-trip time. Under the effect of acoustic fields, τ can be expressed as

$$\tau = \tau_0 + \delta\tau = \frac{2nL}{c} + \int_o^L \frac{2\delta n(z)}{c} \, dz, \quad (45)$$

where $\tau_0 = 2nL/c$ is the constant part and $\delta\tau$ is a variable part resulting from the compression of the propagation medium that induces a refractive index change δn when the propagating acoustic wave overlaps with the laser beam. The system, as demonstrated, can cope with imaging propagation of sound waves as the acoustic field interacts with the environment. This method has the distinct advantage of simplicity, as it requires only a commercial laser diode, a collimating lens, and a light reflector, with minimal electronics and signal processing in order to realize the imaging of the acoustic field.

Physical quantities are of significance in various fields. By applying the precise measurement results of laser feedback interferometers, accuracy in physical quantities can be improved to a higher level, which is beneficial for future applications.

6 Laser Feedback Technology Applications in Other Fields

Although precise measurements in metrology, laser parameters, and physical quantities are significant, there are various targets in industrial and research situations for which measurement cannot be scaled as accurate values. Laser feedback interferometers also has attractive performance in these fields due to their ultrahigh sensitivity and accuracy. Some typical applications are described below.

6.1 Confocal Tomography and Imaging

Imaging objects in a diffusing environment and imaging diffusing objects in three directions are attracting more and more research attention. The optical tomography technique is widely applied in imaging of biological tissues, undersea visibility, and three-dimensional imaging. However, due to the rapid decrease of the backscattering intensity as the detection depth increases, the method has limits in resolution and penetration depth. Lacot et al.[128] proposed laser optical feedback tomography, which can realize the imaging of a French coin immersed in 1 cm of milk using the high sensitivity of the laser feedback effect, the defocus effect on the
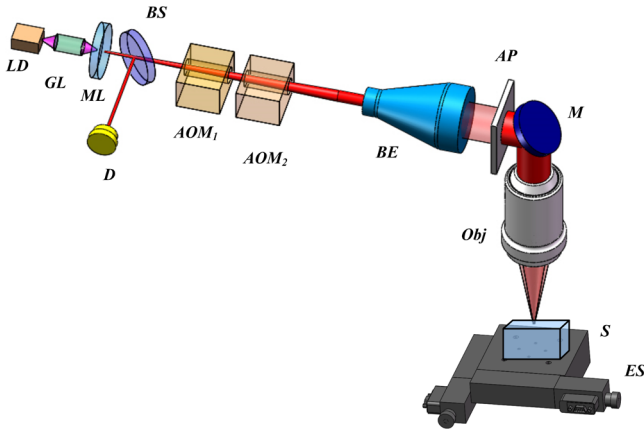
Fig. 15 Schematic of laser confocal feedback tomography. LD, laser diode; GL, grin lens; ML, microchip laser; BS, beam splitter; D, detector; AOMs, acousto-optic modulators; BE, beam expander; AP, annular pupil; Obj, objective lens; S, sample; ES, two-dimensional movement stage.

intensity modulation amplitude, and the resonant enhancement of the intensity modulation amplitude by tuning the frequency shift toward the relaxation oscillation frequency is revealed. Sekine et al.[129] performed the transmission type of self-mixing optical confocal tomography in a highly scattering medium by utilizing the high sensitivity in a solid-state laser. Due to the ultrahigh sensitivity in the laser frequency shift feedback interferometer, combining the technique of confocal tomography, laser confocal feedback tomography is proposed by Tan et al.[130,131] The method employs the axial positioning ability of confocal microscopy. The schematic diagram is shown in Fig. 15.

The resolution of the system is verifiable. The vertical resolution can be evaluated by scanning the defocus response curve and measuring its full width at half maximum (FWHM). From the experiments, the FWHM of the defocus response curve is about 13 μm. The lateral resolution is verified by using a standard grating. The lateral resolution can be obtained to about 1 μm by image analysis of the step. The system has been proved with high resolution and recognition capability of different structures and tissues. Also, due to the ultrahigh sensitivity in the system, the detection capability has reached a high depth. The system can be applied in measuring the structures of microelectromechanical system

devices.[132] The measured etching depth of the largest trench is 90 μm with the width of 350 μm, which is consistent with the manufacturing requirements.

Tissues such as foam and onion inside water can also be measured by the laser confocal feedback system, as shown in Fig. 16. The onion is put into water to avoid the deformation induced by dehydration.

A pin tip is inserted inside the onion to show the significant improvement in detection depth; from the results, the penetration depth inside the onion can reach 2.5 mm.[133] Wang et al.[134] proposed a method for microstructure measurement based on the laser confocal feedback system. The linear relationship between the optical feedback light amplitude and the defocusing amount is calibrated. When scanning the sample in the lateral direction, the amplitude of the feedback light scattered by the sample changes with the sample structure. By comparing the detected feedback light amplitude with the calibrated linear range, the structure can be measured. The accurate measurement of the step height etched in the grating proves its high resolution and absolute positioning in a nonambiguous range of about 10 μm.[135]

From the results, it can be seen that the confocal tomography technique has the capability to realize in-depth structure measurement of microstructured components with high sensitivity.

Considering that there are urgent demands for three-dimensional imaging of the target surfaces as well, many techniques emerge. The advantage of the resonant sensitivity of a short-cavity laser to frequency-shifted optical feedback for highly sensitive detection makes it ideal for surface and volume measurements of noncooperative targets.[136] As a result, the confocal tomography method is also applicable in three-dimensional imaging. Rapid depth scanning is made possible by the use of an electrically controlled variable-focus lens. A variable-focus lens can be manufactured to have a diameter ranging from a few hundred micrometers to 10 mm. This cheap and simple device can be used in any orientation and has good resistance to vibration and shock.[137] With a variable-focus lens, the depth range can be as high as 15 mm, with a precision of 100 μm. The scanning time could be reduced by several orders of magnitude with the use of an array of microchip lasers. The method has potential for fast imaging in three dimensions, but the imaging characteristics remain on the surfaces of the target.

From the two main application directions mentioned above, it can be seen that confocal tomography has the
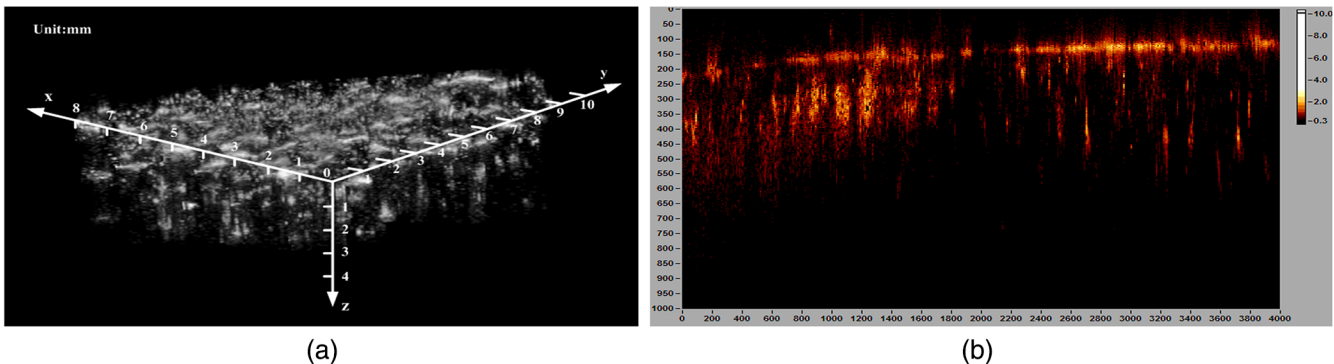

Fig. 16 Tissues measurement in the laser confocal feedback system. (a) Two-dimensional scanning image of foam and (b) image of onion inside water.

capability to measure both the inner structure and the surface characteristics of objects. With the detection depth improving, biological tissues can be measured further.

The laser frequency shift feedback interferometer can also be employed for cell imaging.[138]

It can be deduced that the laser feedback interferometer is well adapted for biological tissues observation on a cellular scale. The system is easily adaptable on a classical microscope, and the laser feedback interferometer images show good contrast, revealing new information compared to other traditional microscopy techniques, in particular, with respect to the relief of the sample without addition of a contrast agent. Hugon et al.[139] combined the information in both magnitude signals and phase signals to improve measurement accuracy. Jacquin et al.[140] presented a laser feedback interferometer device insensitive to optical parasitic reflection, avoiding the adverse effect caused by a parasite in the optical system on amplitude and phase images.

6.2 Sound Reproduction

Similar to the work reported in vibration measurement based on the laser feedback interferometer, the vibration caused by sound propagation can also be measured and used for sound reproduction. Nanometer vibration analysis of a target has been demonstrated by a self-aligned optical feedback vibrometry that uses a laser-diode-pumped microchip solid-state laser by Abe et al.[141] The modulated output waveforms are analyzed using Hilbert transformation. The light intensity feedback ratio can be adjusted using a variable attenuator. Experimental signal characteristics can be well reproduced by numerical simulations. The measurement results at the feedback ratio less than −110 dB obtained by the present technique may enable us to perform *in situ* analyses of, e.g., moving or vibrating targets embedded in optically diffusive media, tissue biomonitoring, cooled atoms, and earthquakes. The almost inaudible sound of music from a speaker below a 20-dB sound pressure level can be clearly reproduced by the present optical microphone.

A high-accuracy fiber optical microphone (FOM) is also applied by a self-mixing technique in a distributed Bragg reflector (DBR) fiber laser based on a nanothick silver diaphragm by Du et al.[142] The nanothick silver diaphragm fabricated by the convenient and low-cost electroless plating method functions as a sensing diaphragm due to its critical susceptibility to air vibration. Simultaneously, the microvibration theory model of self-mixing interference FOM is deduced based on the quasianalytical method. The dynamic property to frequencies and amplitudes is experimentally carried out to characterize the fabricated FOM. The reproduced sound of speech and music can be clearly heard by the human ear, which shows the technique proposed guarantees steady, high signal-to-noise ratio operation and outstanding accuracy in the DBR fiber laser, which has potential for medical and security applications such as real-time voice reproduction for speech and voiceprint verification.

Lu et al.[143] investigated the laser feedback interferometer based on a Er^{3+}-Yb^{3+} DBR fiber laser. It can provide a remote measurement of the displacement and the vibration up to 20 km, which shows the potential for remote sound reproduction. Accurate sound reproduction has significant value in the military field.

6.3 Random Bit Generator and Chaos

Random bit generators are crucial in Monte-Carlo simulation, stochastic modeling, the generation of classical and quantum cryptographic keys, and the random initialization of variables in cryptographic protocols. The existing physical generators based on stochastic noise sources have been limited in bandwidth to ~100 MHz/s generation rates. A physical random bit generator based on a chaotic semiconductor laser with high generation rate is proposed by Kanter et al.[144]

By employing the time-delayed laser feedback effect, the method uses a high derivative of the digitized chaotic laser intensity and generates the random sequence by retaining a number of the least significant bits of the high derivative value. The method is insensitive to laser operational parameters and eliminates the necessity for all external constraints, such as incommensurate sampling rates and laser external cavity round trip time. The generation rate can be as high as 300 GHz/s. Zhang et al.[145] proposed a scheme for enhancing the bandwidth of optical chaotic signals generated from a Fabry–Pérot laser diode with optical feedback using dual-wavelength optical injection and demonstrated experimentally the generation of a broadband chaotic laser up to 32.3 GHz by this method, which can also be applied as the random bit generator.

The demand for increasing security in data exchange using the technology of optical communication networks has directed a considerable part of research to physical layer data encryption techniques.[146] Synchronization in nonlinear and chaotic systems has established a revolutionary approach in securing data communications over fiber transmission, by encoding the messages over chaotic optical carriers. The laser diodes or semiconductor lasers are numerously applied in generating optical chaos.[147] External optical feedback is the most prominent configuration in applications using laser diode chaos with respect to the laser internal timescale and the sensitivity of the phase to the returning field, creating various dynamic methods leading to chaos in large frequency bandwidth.[148] The feedback can be provided by simply adding an external mirror or adding additional components, such as diffraction gratings,[149] polarizers,[150] or wave plates,[151] proving multiple promising ways to produce and control chaos.

The above applications give a brief view of laser feedback interferometry used in other fields. With the growing demands of measurement in various fields, the application of laser feedback interferometry will be explored further.

7 Summary

In this paper, an overview of laser feedback technology is presented. The theoretical analysis is carried out with both the Lang–Kobayashi model and the three mirror model. In particular, the effects of frequency shift feedback and polarization shift feedback are introduced and researched. Due to the autodyne nature in the laser feedback effect, the laser itself can be used as the detector and does not need the reference beam, and the optical paths do not need additional optical components such as isolators, beam splitters, or target mirrors. The signals detected by photodetectors can be easily collected and modulated, simplifying the structure and reducing disturbance noise and cost as well. Some of the optical systems in the paper are complicated, and the cost to build them is high. But these systems are aiming at

specific targets, such as little zero drift, high robustness, high measurement accuracy, or capability for measuring some targets that cannot be easily measured by other methods or techniques. The feedback phenomena can be found in various kinds of lasers, which greatly expands its applications.

The laser feedback effect can be applied in a great range of fields such as metrology, laser parameters measurement, physical quantities measurement, and others. Some of the typical and significant applications are introduced and explored in the body of the overview. The basic principle, the system configurations, and measured results are revealed as well. Hopefully, the representative examples can be employed and transferred in future research in the field of laser feedback.

Laser feedback interferometry has great potential to be exploited in further study. With the fast development in lasers and related technologies, laser feedback can be developed to meet the various specific demands of measurement.

Acknowledgments

References

1. S. Zhang and W. Holzapfel, *Orthogonal Polarization in Lasers: Physical Phenomena and Engineering Applications*, John Wiley & Sons, New York (2013).
2. S. Zhang, *Principle of Orthogonally Polarized Laser*, Tsinghua University Press, Beijing, China (2005).
3. Y. Tan et al., "Response of microchip solid-state laser to external frequency-shifted feedback and its applications," *Sci. Rep.* **3**, 2912 (2013).
4. P. G. R. King and G. J. Steward, "Metrology with an optical maser," *New Sci.* **17**, 180 (1963).
5. T. Taimre et al., "Laser feedback interferometry: a tutorial on the self-mixing effect for coherent sensing," *Adv. Opt. Photonics* **7**(3), 570–631 (2015).
6. C. Hilsum and P. G. R. King, "Some demonstrations of the properties of optical masers," *Contemp. Phys.* **4**, 435–444 (1963).
7. P. G. R. King and G. J. Steward, "Apparatus for measurement of lengths and of other physical parameters which are capable of altering an optical path length," Patent No. 3,409,370 GB Patent 44 192/62 (1968).
8. Y. Mitsuhashi and J. Shimada, "Self-coupled optical pickup," *Opt. Commun.* **17**, 95–97 (1976).
9. K. Otsuka, "Highly sensitive measurement of Doppler-shift with a microchip solid-state laser," *Jpn. J. Appl. Phys.* **31**(11), L1546–L1548 (1992).
10. Y. Tan et al., "Power spectral characteristic of a microchip Nd:YAG laser subjected to frequency-shifted optical feedback," *Laser Phys. Lett.* **10**(2), 025001 (2013).
11. G. Giuliani et al., "Laser diode self-mixing technique for sensing applications," *J. Opt. A: Pure Appl. Opt.* **4**, S283–S294 (2002).
12. J. von Staden, T. Gensty, and W. Elsäßer, "Measurements of the α factor of a distributed-feedback quantum cascade laser by an optical feedback self-mixing technique," *Opt. Lett.* **31**(17), 2574–2576 (2006).
13. R. P. Green et al., "Linewidth enhancement factor of terahertz quantum cascade lasers," *Appl. Phys. Lett.* **92**(7), 071106 (2008).
14. K. Bertling et al., "Demonstration of the self-mixing effect in interband cascade lasers," *Appl. Phys. Lett.* **103**(23), 231107 (2013).
15. H. Hao et al., "Micro-displace sensor based on self-mixing interference of the fiber laser with phase modulation," *Photonics Sens.* **4**(4), 379–384 (2014).
16. X. Dai et al., "Self-mixing interference in fiber ring laser and its application for vibration measurement," *Opt. Express* **17**(19), 16543–16548 (2009).
17. L. Gelens et al., "Excitability in semiconductor microring lasers: experimental and theoretical pulse characterization," *Phys. Rev. A* **82**, 063841 (2010).
18. D. O. Brien et al., "Feedback sensitivity of 1.3 m InAs/GaAs quantum dot lasers," *Electron. Lett.* **39**(25), 1819–1820 (2003).
19. S. Donati, "Developing self-mixing interferometry for instrumentation and measurements," *Laser Photonics Rev.* **6**(3), 393–417 (2012).
20. R. Lang and K. Kobayashi, "External optical feedback effects on semiconductor injection laser properties," *IEEE J. Quantum Electron.* **16**(3), 347–355 (1980).
21. M. B. Spencer and W. E. Lamb, "Laser with a transmitting window," *Phys. Rev. A* **5**(2), 884–892 (1972).
22. P. Spencer, P. Rees, and I. Pierce, *Theoretical Analysis in Unlocking Dynamical Diversity: Optical Feedback Effects on Semiconductor Lasers*, John Wiley & Sons, Chichester (2005).
23. C. H. Henry, "Theory of the linewidth of semiconductor lasers," *IEEE J. Quantum Electron.* **18**(2), 259–264 (1982).
24. K. Petermann, *Laser Diode Modulation and Noise*, Kluwer Academic Publishers, Dordrecht, The Netherlands (1991).
25. M. O. Nski and J. Buus, "Linewidth broadening factor in semiconductor lasers-an overview," *IEEE J. Quantum Electron.* **23**, 9–29 (1987).
26. P. J. de Groot, G. M. Gallatin, and S. H. Macomber, "Ranging and velocimetry signal generation in a backscatter-modulated laser diode," *Appl. Opt.* **27**(21), 4475–4480 (1988).
27. G. H. M. van Tartwijk and G. P. Agrawal, "Laser instabilities: a modern perspective," *Prog. Quantum Electron.* **22**, 43–122 (1998).
28. P. J. Brannon, "Laser feedback: Its effect on laser frequency," *Appl. Opt.* **15**(5), 1119–1120 (1976).
29. S. Zhang et al., "Spectrum broadening in optical frequency-shifted feedback of microchip laser," *IEEE Photonics Technol. Lett.* **28**(14), 1593–1596 (2016).
30. W. Koechner, *Solid-State Laser Engineering*, Springer-Verlag, New York (2006).
31. Y. Tan and S. Zhang, "Self-mixing interference effects of microchip Nd: YAG laser with a wave plate in the external cavity," *Appl. Opt.* **46**(24), 6064–6068 (2007).
32. P. Zhang et al., "Measurement method for optical retardation based on the phase difference effect of laser feedback fringes," *Appl. Opt.* **54**(2), 204–209 (2015).
33. P. Zhang et al., "Phase difference in modulated signals of two orthogonally polarized outputs of a Nd: YAG microchip laser with anisotropic optical feedback," *Opt. Lett.* **38**(21), 4296–4299 (2013).
34. Y. Tan et al., "Self-mixing interference effects in orthogonally polarized dual-frequency Nd: YAG lasers at different feedback levels," *Appl. Phys. B* **95**(4), 731–737 (2009).
35. Y. Wu et al., "A sensitive method of determining optic axis azimuth based on laser feedback," *Chin. Phys. B* **22**(12), 124205 (2013).
36. Y. Wu et al., "Note: high-performance HeNe laser feedback interferometer with birefringence feedback cavity scanned by piezoelectric transducer," *Rev. Sci. Instrum.* **84**(5), 056103 (2013).
37. M. Norgia and S. Donati, "A displacement-measuring instrument utilizing self-mixing interferometry," *IEEE Trans. Instrum. Meas.* **52**(6), 1765–1770 (2003).
38. S. Zhang, Y. Tan, and S. Zhang, "Note: measurement speed improvement of microchip Nd:YAG laser feedback interferometer," *Rev. Sci. Instrum.* **85**(3), 036112 (2014).
39. S. Zhang et al., "A microchip laser feedback interferometer with nanometer resolution and increased measurement speed based on phase meter," *Appl. Phys. B* **116**(3), 609–616 (2014).
40. S. Zhang et al., "A microchip laser source with stable intensity and frequency used for self-mixing interferometry," *Rev. Sci. Instrum.* **87**(5), 053114 (2016).
41. Y. Tan, S. Zhang, and Y. Zhang, "Laser feedback interferometry based on phase difference of orthogonally polarized lights in external birefringence cavity," *Opt. Express* **17**(16), 13939–13945 (2009).
42. J. Li, Y. Tan, and S. Zhang, "Generation of phase difference between self-mixing signals in a-cut Nd:YVO₄ laser with a wave plate in the external cavity," *Opt. Lett.* **40**(15), 3615–3618 (2015).
43. D. Guo, M. Wang, and H. Hao, "Displacement measurement using a laser feedback grating interferometer," *Appl. Opt.* **54**(13), 9320–9325 (2015).
44. O. D. Bernal et al., "Robust fringe detection based on bi-wavelet transform for self-mixing displacement sensor," in *IEEE Sensors* (2015).
45. S. Donati, D. Rossi, and M. Norgia, "Single channel self-mixing interferometer measures simultaneously displacement and tilt and yaw angles of a reflective target," *IEEE J. Quantum Electron.* **51**(12), 1–8 (2015).
46. Z. Zeng et al., "High-accuracy self-mixing interferometer based on single high-order orthogonally polarized feedback effects," *Opt. Express* **23**(13), 16977–16983 (2015).
47. Y. Tan et al., "Method for in situ calibration of multiple feedback interferometers," *Chin. Opt. Lett.* **11**(10), 102601–102603 (2013).
48. A. Jha, F. J. Azcona, and S. Royo, "Frequency-modulated optical feedback interferometry for nanometric scale vibrometry," *IEEE Photonics Technol. Lett.* **28**(11), 1217–1220 (2016).
49. J. Chen et al., "Synthetic-wavelength self-mixing interferometry for displacement measurement," *Opt. Commun.* **368**, 73–80 (2016).
50. Y. Tao, M. Wang, and W. Xia, "Semiconductor laser self-mixing micro-vibration measuring technology based on Hilbert transform," *Opt. Commun.* **368**, 12–19 (2016).
51. R. C. Addy et al., "Effects of external reflector alignment in sensing applications of optical feedback in laser diodes," *J. Lightwave Technol.* **14**(12), 2672–2676 (1996).

52. C. Jiang, Z. Zhang, and C. Li, "Vibration measurement based on multiple self-mixing interferometry," *Opt. Commun.* **367**, 227–233 (2016).
53. A. Magnani et al., "Self-mixing digital closed-loop vibrometer for high accuracy vibration measurements," *Opt. Commun.* **365**, 133–139 (2016).
54. S. Wu et al., "Simultaneous measurement of vibration amplitude and rotation angle based on a single-channel laser self-mixing interferometer," *Chin. Opt. Lett.* **14**(2), 021201 (2016).
55. A. N. Lukashkin, M. E. Bashtanov, and I. J. Russell, "A self-mixing laser-diode interferometer for measuring basilar membrane vibrations without opening the cochlea," *J. Neurosci. Methods* **148**(2), 122–129 (2005).
56. G. Giuliani, S. Bozzi-Pietra, and S. Donati, "Self-mixing laser diode vibrometer," *Meas. Sci. Technol.* **14**, 24–32 (2003).
57. Y. Huang et al., "A study of vibration system characteristics based on laser self-mixing interference effect," *J. Appl. Phys.* **112**(2), 023106 (2012).
58. M. Chen et al., "Damping microvibration measurement using laser diode self-mixing interference," *IEEE Photonics J.* **6**(3), 1–8 (2014).
59. S. Shinohara et al., "Compact and high-precision range finder with wide dynamic range and its application," *IEEE Trans. Instrum. Meas.* **41**(1), 40–44 (1992).
60. E. Gagnon and J. Rivest, "Laser range imaging using the self-mixing effect in a laser diode," *IEEE Trans. Instrum. Meas.* **48**(3), 693–699 (1999).
61. K. Kou et al., "Injected current reshaping in distance measurement by laser self-mixing interferometry," *Appl. Opt.* **53**(27), 6280–6286 (2014).
62. H. Moench et al., "VCSEL based sensors for distance and velocity," *Proc. SPIE* **9766**, 97660A (2016).
63. R. Michalzik, *VCSELs Fundamentals, Technology and Applications of Vertical-Cavity Surface-Emitting Lasers*, Springer, Germany (2012).
64. F. Gouaux, N. Servagent, and T. Bosch, "Three-dimensional object construction using a self-mixing type scanning laser range finder," *Appl. Opt.* **37**(28), 6684–6689 (1998).
65. D. Guo, M. Wang, and H. Xiang, "Self-mixing interferometry based on a double-modulation technique for absolute distance measurement," *Appl. Opt.* **46**(9), 1486–1491 (2007).
66. M. J. Rudd, "A laser Doppler velocimeter employing the laser as a mixer-oscillator," *J. Phys. E* **1**(7), 723–726 (1968).
67. P. J. de Groot and G. M. Gallatin, "Backscatter-modulation velocimetry with an external-cavity laser diode," *Opt. Lett.* **14**(3), 165–167 (1989).
68. M. H. Koelink et al., "Laser Doppler velocimeter based on the self-mixing effect in a fiber-coupled semiconductor laser: theory," *Appl. Opt.* **31**(18), 3401–3408 (1992).
69. E. T. Shimizu, "Directional discrimination in the self-mixing type laser Doppler velocimeter," *Appl. Opt.* **26**(21), 4541–4544 (1987).
70. S. Shinohara et al, "Compact and versatile self-mixing type semiconductor laser Doppler velocimeters with direction-discrimination circuit," *IEEE. Trans. Instrum. Meas.* **38**(2), 574–577 (1989).
71. O. Mikami and C. Fujikawa, "Laser diode Doppler velocimeter with 3-beams and self-mixing effect enabling 3-diminsional velocity measurement," *Proc. SPIE* **9899**, 989922 (2016).
72. L. Scalise et al., "Self-mixing laser diode velocimetry: application to vibration and velocity measurement," *IEEE Trans. Instrum. Meas.* **53**(1), 223–232 (2004).
73. T. Bosch et al., "The self-mixing interference inside a laser diode: application to displacement, velocity and distance measurement," *Proc. SPIE* **3478**, 98–108 (1998).
74. R. Kliese and A. D. Rakić, "Spectral broadening caused by dynamic speckle in self-mixing velocimetry sensors," *Opt. Express* **20**(17), 18757–18771 (2012).
75. D. Han, M. Wang, and J. Zhou, "Fractal analysis of self-mixing speckle signal in velocity sensing," *Opt. Express* **16**(5), 3204–3211 (2008).
76. W. Huang et al., "Effect of angle of incidence on self-mixing laser Doppler velocimeter and optimization of the system," *Opt. Commun.* **281**(6), 1662–1667 (2008).
77. S. K. Özdemir et al., "A speckle velocimeter using a semiconductor laser with external optical feedback from a moving surface: effects of system parameters on the reproducibility and accuracy of measurements," *Meas. Sci. Technol.* **11**(10), 1447–1455 (2000).
78. S. K. Özdemir et al., "Correlation-based speckle velocimeter with self-mixing interference in a semiconductor laser diode," *Appl. Opt.* **38**(33), 6859–6865 (1999).
79. S. K. Özdemir et al., "Simultaneous measurement of velocity and length of moving surfaces by a speckle velocimeter with two self-mixing laser diodes," *Appl. Opt.* **38**(10), 1968–1974 (1999).
80. S. Shinohara et al., "Compact optical instrument for surface classification using self-mixing interference in a laser diode," *Opt. Eng.* **40**(1), 38–43 (2001).
81. A. Alexandrova and C. P. Welsch, "Laser diode self-mixing technique for liquid velocimetry," *Nucl. Instrum. Methods Phys. Res. A* **830**, 497–503 (2016).
82. L. Campagnolo et al., "Flow profile measurement in microchannel using the optical feedback interferometry sensing technique," *Microfluid. Nanofluid.* **14**(1–2), 113–119 (2013).
83. E. E. Ramírez-Miquet et al., "Optical feedback interferometry for velocity measurement of parallel liquid-liquid flows in a microchannel," *Sensors* **16**(8), 1233 (2016).
84. S. K. Ozdemir et al., "Self-mixing laser speckle velocimeter for blood flow measurement," *IEEE. Trans. Instrum. Meas.* **49**(5), 1029–1035 (2000).
85. F. F. M. de Mul et al., "Self-mixing laser-Doppler velocimetry of liquid flow and of blood perfusion in tissue," *Appl. Opt.* **31**(27), 5844–5851 (1992).
86. M. Slot et al., "Blood flow velocity measurements based on the self-mixing effect in a fibre-coupled semiconductor laser: *in vivo* and *in vitro* measurements," *Med. Biol. Eng. Comput.* **30**(4), 441–446 (1992).
87. K. Mito et al., "Self-mixing effect of the semiconductor laser Doppler method for blood flow measurement," *Med. Biol. Eng. Comput.* **31**(3), 308–310 (1993).
88. I. Ohno and S. Shinohara, "A comparative study for the assessment on blood flow measurement using self-mixing laser speckle interferometer," *IEEE. Trans. Instrum. Meas.* **57**(2), 355–363 (2008).
89. S. Shinohara, S. Takamiya, and H. Yoshida, "Noninvasive blood flow measurement using speckle signals from a self-mixing laser diode: *in vitro* and *in vivo* experiments," *Opt. Eng.* **39**(9), 2574–2580 (2000).
90. M. Norgia, A. Pesatori, and S. Donati, "Compact laser-diode instrument for flow measurement," *IEEE. Trans. Instrum. Meas.* **65**(6), 1478–1483 (2016).
91. E. Figueiras et al., "Self-mixing microprobe for monitoring microvascular perfusion in rat brain," *Med. Biol. Eng. Comput.* **51**(1–2), 103–112 (2013).
92. Y. Zhao et al., "Self-mixing fiber ring laser velocimeter with orthogonal-beam incident system," *IEEE Photonics J.* **6**(2), 1–11 (2014).
93. H. Matsumoto, "Alignment of length-measuring IR laser interferometer using laser feedback," *Appl. Opt.* **19**(1), 1–2 (1980).
94. S. Zhang, Y. Tan, and S. Zhang, "Non-contact angle measurement based on parallel multiplex laser feedback interferometry," *Chin. Phys. B* **23**(11), 114202 (2014).
95. C. Ren, Y. Tan, and S. Zhang, "External-cavity birefringence feedback effects of microchip Nd:YAG laser and its application in angle measurement," *Chin. Phys. B* **18**(8), 3438–3443 (2009).
96. G. Giuliani, S. Donati, and M. Passerini, "Angle measurement by injection-detection in a laser diode," *Opt. Eng.* **40**(1), 95–99 (2001).
97. I. Zhong et al., "High-precision small-angle measurement based on laser self-mixing interference," in *Frontiers in Optics*, Optical Society of America (2010).
98. Y. Tan and S. Zhang, "Linearly polarized dual frequency Nd:YAG lasers with tunable frequency difference and its application in precision angle measurement," *Chin. Phys. Lett.* **24**(9), 2590–2593 (2007).
99. M. T. Fathi and S. Donati, "Simultaneous measurement of thickness and refractive index by a single-channel self-mixing interferometer," *IET Optoelectron.* **6**(1), 7–12 (2011).
100. I. Xu et al., "Simultaneous measurement of refractive-index and thickness for optical materials by laser feedback interferometry," *Rev. Sci. Instrum.* **85**(8), 083111 (2014).
101. Y. Tan and K. Zhu, "Lens thickness measurement and axial positioning method based on the frequency-shifted confocal feedback," in *Conf. on Lasers and Electro-Optics (CLEO)* (2016).
102. Y. Tan, K. Zhu, and S. Zhang, "New method for lens thickness measurement by the frequency-shifted confocal feedback," *Opt. Commun.* **380**, 91–94 (2016).
103. G. Giuliani, M. Norgia, and S. Donati, "Laser diode linewidth measurement by means of self-mixing interferometry," in *IEEE 12th Annual Meeting on Lasers and Electro-optics Society* (1999).
104. J. Xi, Y. Yu, and T. Bosch, "Estimating the parameters of semiconductor lasers based on weak optical feedback self-mixing interferometry," *IEEE. J. Quantum Electron.* **41**(8), 1058–1064 (2005).
105. Y. Yu, G. Giuliani, and S. Donati, "Measurement of the linewidth enhancement factor of semiconductor lasers based on the optical feedback self-mixing effect," *IEEE Photonics Technol. Lett.* **16**(4), 990–992 (2004).
106. S. Kaya Özdemir, S. Shinohara, and H. Yoshida, "Effect of linewidth enhancement factor on Doppler beat waveform obtained from a self-mixing laser diode," *Opt. Rev.* **7**(6), 550–554 (2000).
107. I. Wei et al., "Linewidth enhancement factor measurement based on optical feedback self-mixing effect: a genetic algorithm approach," *J. Opt. A* **11**, 1–9 (2009).
108. J. von Staden, T. Gensty, and W. Elsäßer, "Measurements of the α factor of a distributed-feedback quantum cascade laser by an optical feedback self-mixing technique," *Opt. Lett.* **31**(17), 2574–2576 (2006).
109. Y. Yu et al., "Toward automatic measurement of the linewidth-enhancement factor using optical feedback self-mixing interferometry with weak optical feedback," *IEEE. J. Quantum Electron.* **43**(7), 527–534 (2007).
110. C. Szwaj, E. Lacot, and O. Hugon, "Large linewidth-enhancement factor in a microchip laser," *Phys. Rev. A* **70**, 033809 (2004).
111. E. Cabrera, O. G. Calderón, and J. M. Guerra, "Experimental evidence of antiphase population dynamics in lasers," *Phys. Rev. A* **72**(4), 043824 (2005).

112. Y. Tan et al., "Measurement of a polarization cross-saturation coefficient in two-mode Nd: YAG lasers by polarized optical feedback," *J. Phys. B* **42**(2), 025401 (2009).
113. I. Xu et al., "Measurement of refractive index ranging from 1.42847 to 2.48272 at 1064 nm using a quasi-common-path laser feedback system," *Chin. Phys. Lett.* **32**(9), 090701 (2015).
114. L. Xu et al., "Refractive index measurement of liquids by double-beam laser frequency-shift feedback," *IEEE Photonics Technol. Lett.* **28**(10), 1049–1052 (2016).
115. L. Fei et al., "Polarization control in a He-Ne laser using birefringence feedback," *Opt. Express* **13**(8), 3117–3122 (2005).
116. W. Chen et al., "Polarization flipping and hysteresis phenomenon in laser with optical feedback," *Opt. Express* **21**(1), 1240–1246 (2013).
117. W. Chen et al., "Semi-classical theory and experimental research for polarization flipping in a single frequency laser with feedback effect," *Chin. Phys. B* **21**(9), 090301 (2012).
118. W. Chen et al., "Measurement of phase retardation of waveplate online based on laser feedback," *Rev. Sci. Instrum.* **83**(1), 013101 (2012).
119. W. Chen, S. Zhang, and X. Long, "Internal stress measurement by laser feedback method," *Opt. Lett.* **37**(13), 2433–2435 (2012).
120. F. Zheng et al., "Study of non-contact measurement of the thermal expansion coefficients of materials based on laser feedback interferometry," *Rev. Sci. Instrum.* **86**(4), 043109 (2015).
121. F. Zheng et al., "The approach of compensation of air refractive index in thermal expansion coefficients measurement based on laser feedback interferometry," *Chin. Phys. Lett.* **32**(7), 070702 (2015).
122. Y. Ding et al., "Measurement of thermal expansion coefficients of materials based on Nd:YVO$_4$ laser feedback systems," *Proc. SPIE* **9524**, 95240L (2015).
123. D. Melchionni and M. Norgia, "Optical system for liquid level measurements," *Rev. Sci. Instrum.* **85**(7), 075113 (2014).
124. D. Melchionni, A. Pesatori, and M. Norgia, "Liquid level measurement system based on a coherent optical sensor," in *Proc. IEEE Int. Instrumentation and Measurement Technology Conference (I2MTC 2014)*, Montevideo (2014).
125. Y. Tan et al., "Real-time liquid evaporation rate measurement based on a microchip laser feedback interferometer," *Chin. Phys. Lett.* **30**(12), 124202 (2013).
126. R. Gamidov, E. Sadikhov, and M. Cetintas, "Optical feedback in diode laser for sound-pressure measurement," *Proc. SPIE* **3411**, 624–629 (1998).
127. K. Bertling et al., "Imaging of acoustic fields using optical feedback interferometry," *Opt. Express* **22**(24), 30346–30356 (2014).
128. E. Lacot, R. Day, and F. Stoeckel, "Laser optical feedback tomography," *Opt. Lett.* **24**(11), 744–746 (1999).
129. T. Sekine, K. Shimizu, and K. Otsuka, "Applying the self-mixing effect of a microchip laser to optical CT," *Proc. SPIE* **4630**, 41 (2002).
130. Y. Tan et al., "Laser confocal feedback tomography and nano-step height measurement," *Sci. Rep.* **3**, 2971 (2013).
131. Y. Tan et al., "Inspecting and locating foreign body in biological sample by laser confocal feedback technology," *Appl. Phys. Lett.* **103**(10), 102101 (2013).
132. C. Xu et al., "The structure measurement of micro-electro-mechanical system devices by the optical feedback tomography technology," *Appl. Phys. Lett.* **102**(22), 221902 (2013).
133. C. Xu et al., "Inner structure detection by optical tomography technology based on feedback of microchip Nd:YAG lasers," *Opt. Express* **21**(10), 11819–11826 (2013).
134. W. Wang et al., "Microstructure measurement based on frequency-shift feedback in a-cut Nd:YVO4 laser," *Chin. Opt. Lett.* **13**(12), 121201–121205 (2015).
135. W. Wang, S. Zhang, and Y. Li, "Surface microstructure profilometry based on laser confocal feedback," *Rev. Sci. Instrum.* **86**(10), 103108 (2015).
136. R. Day et al., "Three-dimensional sensing based on a dynamically focused laser optical feedback imaging technique," *Appl. Opt.* **40**(12), 1921–1924 (2001).
137. K. Otsuka et al., "Real-time nanometer-vibration measurement with a self-mixing microchip solid-state laser," *Opt. Lett.* **27**(15), 1339–1341 (2002).
138. I. Hugon et al., "Cell imaging by coherent backscattering microscopy using frequency-shifted optical feedback in a microchip laser," *Ultramicroscopy* **108**(6), 523–528 (2008).
139. I. Hugon et al., "Coherent microscopy by laser optical feedback imaging (LOFI) technique," *Ultramicroscopy* **111**(11), 1557–1563 (2011).
140. O. Jacquin et al., "Laser optical feedback imaging insensitive to parasitic optical feedback," *App. Opt.* **46**(27), 6779–6782 (2007).
141. K. Abe, K. Otsuka, and J. Ko, "Self-mixing laser Doppler vibrometry with high optical sensitivity: application to real-time sound reproduction," *New J. Phys.* **5**, 8 (2003).
142. Z. Du et al., "High-accuracy fiber optical microphone in a DBR fiber laser based on a nanothick silver diaphragm by self-mixing technique," *Opt. Express* **21**(25), 30580–30590 (2013).
143. L. Lu et al., "Self-Mixing signal in Er^{3+}-Yb^{3+} Co-doped distributed Bragg reflector fiber laser for remote sensing applications up to 20 Km," *IEEE Photonics Technol. Lett.* **24**(5), 392–394 (2012).
144. I. Kanter et al., "An optical ultrafast random bit generator," *Nat. Photonics* **4**, 58–61 (2010).
145. M. Zhang et al., "Generation of broadband chaotic laser using dual-wavelength optically injected Fabry–Pérot laser diode with optical feedback," *IEEE Photonics Technol. Lett.* **23**(24), 1872–1874 (2011).
146. A. Argyris et al., "Photonic integrated device for chaos applications in communications," *Phys. Rev. Lett.* **100**(19), 194101 (2008).
147. M. C. Soriano et al., "Complex photonics: dynamics and applications of delay-coupled semiconductors lasers," *Rev. Mod. Phys.* **85**(1), 421–470 (2013).
148. M. Sciamanna and K. A. Shore, "Physics and applications of laser diode chaos," *Nat. Photonics* **9**(3), 151–162 (2015).
149. M. Giudici et al., "Dynamical behavior of semiconductor lasers with frequency selective optical feedback," *Chaos Solitons Fractals* **10**(4), 811–818 (1999).
150. Y. Hong et al., "The effects of polarization-resolved optical feedback on the relative intensity noise and polarization stability of vertical-cavity surface-emitting lasers," *J. Lightwave Technol.* **24**(8), 3210–3216 (2006).
151. H. Li et al., "Stable polarization self-modulation in vertical-cavity surface-emitting lasers," *Appl. Phys. Lett.* **72**(19), 2355–2357 (1998).

Jiyang Li received his bachelor's degree in electrical engineering and its automation from Beihang University in 2012. He is a PhD candidate at the Beihang University whose major is optical engineering. His research interests are mainly in research and design of novel optical instruments and interferomic measurement technology.

Haisha Niu is a PhD candidate at the Beihang University whose major is optical engineering. Her research interests are mainly in research and design of novel optical instruments and birefringence measurement technology.

Yanxiong Niu received his doctor degree in physical electronics from Tianjin University and his postdoctoral degree in optical engineering from Tsinghua University. He is a professor and a PhD tutor at the Beihang University. His research interests are mainly in research and design of novel optical instruments and optoelectronic countermeasure technology.